Rockefeller University
Report No. COO-2232A-79

RECENT HIGH p_T RESULTS FROM THE CERN ISR

Michael J. Tannenbaum
The Rockefeller University
New York, N.Y. 10021
U.S.A.

ABSTRACT

Significant new results have been presented this past year on the subjects of high p_T π^0 production and the properties of jets in proton-proton collisions.

Paper Presented to the XIVth Rencontre de Moriond Conference
11 - 17 March 1979, Les Arcs, Savoie, France

I - INTRODUCTION

Most of the results that I shall review in this talk were first presented in calendar year 1978, with a distinct surge at the time of the XIX International Conference in Tokyo at the end of August. For people who are not familiar with the experimental results and folklore of the "Classical" period of high p_T physics (1972-1977), a review of this period, which will serve as an introduction to this talk, can be found in the Proceedings of the Meeting in Marseilles, 1978 [1].

II - INCLUSIVE CROSS SECTIONS AT HIGHER p_T

In an inclusive measurement, the number of particles, Δn, at a given transverse momentum p_T, in an interval Δp_T, is counted for a given integrated luminosity $\mathcal{L}$, and the invariant cross section is computed:

$$E\frac{d^3\sigma}{dp^3} = \frac{d^3\sigma}{p_T dp_T dy d\phi} = \frac{1}{\mathcal{L}}\frac{\Delta n}{\Delta p_T}\frac{1}{p_T}\frac{1}{\Delta y\,\Delta\phi} \qquad (1)$$

The factor $\Delta y\,\Delta\phi$ is the acceptance, or solid angle of the detector. ϕ is the azimuthal angle of the detected particle, and y is its rapidity which is related to the longitudinal momentum, or polar angle:

$$y = \ln\frac{E + p_L}{\sqrt{p_T^2 + m^2}} \approx -\ln\tan\theta/2.$$

For simplicity, all quantities are taken in the center-of-mass system, of total energy $\sqrt{s}$. Two other useful variables are the scaled transverse and longitudinal momenta

$$x_T = 2p_T/\sqrt{s}$$

$$\text{Feynman}\quad x = 2p_L/\sqrt{s}$$

The experimental results [2-5] on the inclusive production of pions near 90^0 C.M. in proton-proton collisions of center-of-mass energies $\sqrt{s}$ between 20 and 60 GeV, and transverse momenta p_T between 2 and 7 GeV/c, can be parameterized by the scaling form

$$E\frac{d^3\sigma}{dp^3} = \frac{1}{p_T^{\,n}}F(x_T) \qquad (2)$$

with $n \approx 8$ and $F(x_T) = A(1 - x_T)^m$, with $m \approx 10$. This scaling form (2) was originally suggested by models [6-10] in which particle production at large p_T is the result of hard scattering of hadronic constituents at small distances. The parameter n is related to the type of constituents and the force law that

governs their scattering. For instance, electromagnetic scattering of point constituents [6] or asymptotically free vector gluon exchange [11] would give n=4; while quark-meson scattering via the exchange of a quark [7] would give n=8, as apparently observed. Recent theoretical work [12-16] based on QCD predicts that the scaling form (2) is not valid, and that the invariant cross section should approach the p_T^{-4} law as p_T is increased at a fixed value of x_T.

Two ISR experiments this year have published results [17,18] on inclusive π^0 production near 90° in proton-proton collisions, in a new p_T range, $7.0 \leq p_T \leq 14.0$ GeV/c.

The apparatus of the CERN-Saclay-Zurich collaboration [17], shown in Figure 1, consists basically of a large array of lead glass Cerenkov counters, with a solid angle of $\Delta\Omega = 0.6$ steradians located at 90° in the C.M. system. A charged particle spectrometer made of drift chambers and an analyzing magnet precedes the lead glass array and determines the azimuthal aperture of $\Delta\phi = \pm 15°$.

If the scaling form for inclusive π^0 production is valid, then equation (2) can be rewritten as

$$E \frac{d^3\sigma}{dp^3} = \frac{1}{(\sqrt{s})^n} G(x_T) \quad . \tag{3}$$

In this formulation, a plot of $E\, d^3\sigma/dp^3$ versus x_T for different values of $\sqrt{s}$ should be a series of universal curves with normalizations proportional to $(\sqrt{s})^{-n}$. At any value of x_T a value of n can be found:

$$(\sqrt{s_2}/\sqrt{s_1})^n = \frac{E \frac{d^3\sigma}{dp^3}(\sqrt{s_1}, x_T)}{E \frac{d^3\sigma}{dp^3}(\sqrt{s_2}, x_T)} \tag{4}$$

If scaling works, then n is unique. If scaling breaks down, then n will be a function of $\sqrt{s_1}$, $\sqrt{s_2}$ and x_T; and a new formulation of the problem will be required.

The CSZ data are shown in Figure 2 for $0.20 \leq x_T \leq 0.45$ and $\sqrt{s}$ = 62 and 52 GeV. Also indicated are data points from Fermilab [5] at $\sqrt{s}$ = 27.4 GeV. The solid lines through the data points represent a fit to the cross section of the form

$$E \frac{d^3\sigma}{dp^3} = \frac{A}{p_T^n} (1 - x_T)^m \tag{6}$$

with $n = 6.6 \pm 0.8$ and $m = 9.6 \pm 1.0$. The authors point out that a similar analysis between their data and the Fermilab data at $\sqrt{s}$ = 27.4 GeV would give $n = 7.3 \pm 0.6$ for the range $0.2 \leq x_T \leq 0.4$.

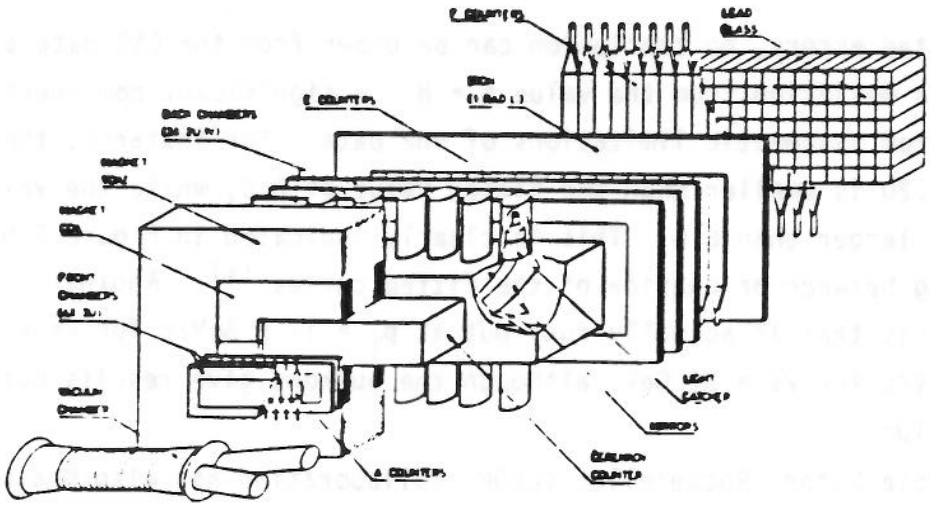

FIG. 1

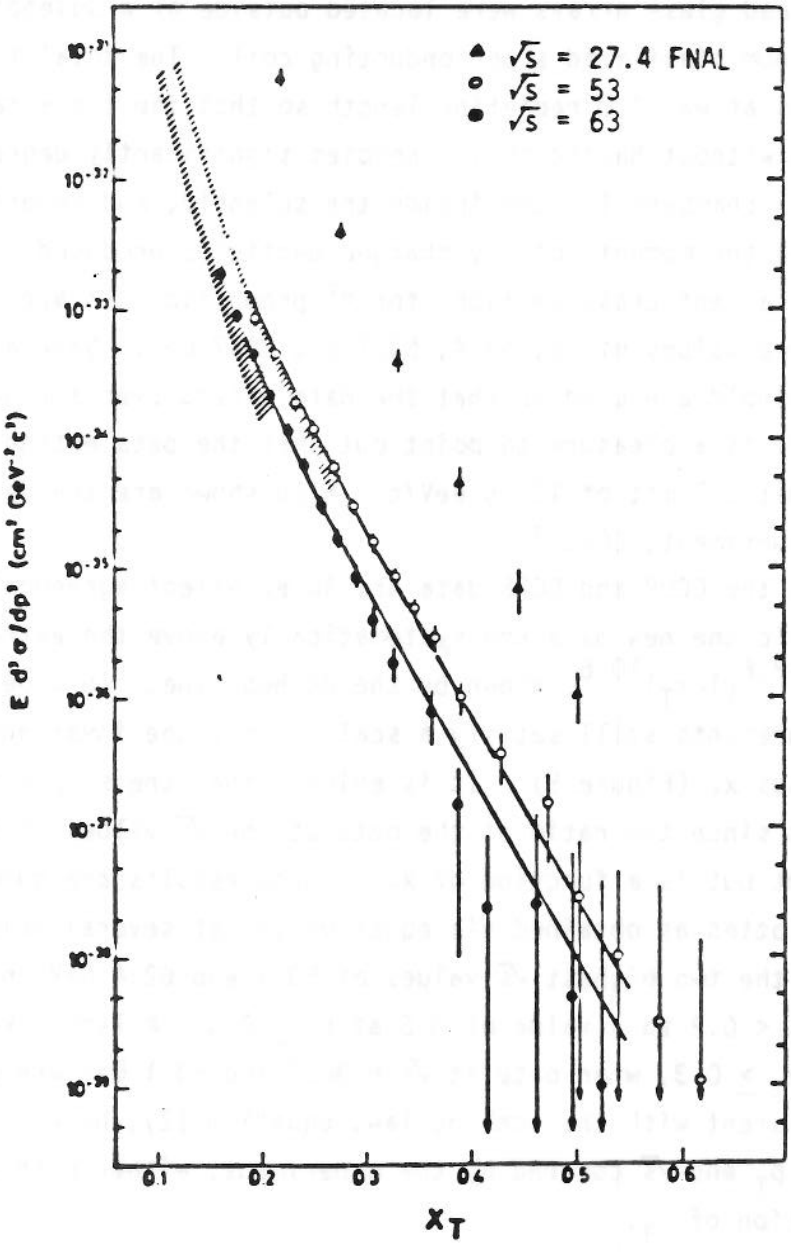
$\sqrt{s}$ = 27.4 FNAL
$\sqrt{s}$ = 53
$\sqrt{s}$ = 63
E d³σ/dp³ (cm² GeV⁻² c³)
10^{-31}
10^{-32}
10^{-33}
10^{-34}
10^{-35}
10^{-36}
10^{-37}
10^{-38}
10^{-39}
0.1
0.2
0.3
0.4
0.5
0.6
x_T

FIG. 2

Within the quoted errors, no conclusion can be drawn from the CSZ data as to whether there is a deviation from the value n = 8. A significant component of the error comes from systematic limitations of the data. For instance, the value of n at $x_T = 0.20$ is smaller than the fitted value of 6.6, while the value of n at $x_T = 0.30$ is larger than 6.6. This is clearly indicated in Figure 2 by the data points lying between or outside of the fitted curves [19]. Another comment on this data is that it actually runs out at $p_T = 11.5$ GeV/c for $\sqrt{s} = 62$ GeV and $p_T = 12.5$ GeV/c for $\sqrt{s} = 52$ GeV, although the authors give results out to much larger p_T values.

The CERN-Columbia-Oxford-Rockefeller (CCOR) collaboration has also measured higher p_T π^0 production at the ISR [18] using two large lead glass arrays, each of solid angle $\Delta\Omega = 1$ steradian ($\Delta\theta = \pm 31^0$, $\Delta\phi = \pm 27$), at 90^0 in the C.M. system (Figure 3). The lead glass arrays were located outside of a solenoid magnet made with an aluminum stabilized superconducting coil. The total thickness of the coil and cryostat was 1.0 radiation length so that the two γ rays from a π^0 could penetrate without having their energies significantly degraded. A set of cylindrical drift chambers located inside the solenoid, and covering the full azimuth, measured the momenta of any charged particles produced.

In Figure 4, the invariant cross sections for π^0 production [20] are plotted versus p_T for three values of $\sqrt{s}$, 62.4, 53.1 and 30.7 GeV. Several values of triggering threshold are used so that the data extend over a range of $3.5 \leq p_T \leq 14.0$ GeV/c. It is a pleasure to point out that the data extend well beyond the Fermilab kinematic limit of 12.75 GeV/c. Also shown are the data and best fit of a previous experiment, CCRS [3].

For $p_T < 6.0$ GeV/c, the CCOR and CCRS data are in excellent agreement. However, for $p_T > 7.0$ GeV/c the new data are systematically above the extrapolation of the CCRS fit, $p_T^{-8.6}(1-x_T)^{10.6}$, shown by the dashed line. In order to see whether the new measurements still satisfy a scaling law, the invariant cross sections are plotted versus x_T (Figure 5). It is evident that the simple scaling law of equation (3) fails since the ratio of the data at the $\sqrt{s}$ values of 53.1 and 62.4 is not a constant but is a function of x_T. These results are summarized in Figure 6 where n is plotted as obtained via equation (4) at several values of x_T [21]. For the data at the two highest $\sqrt{s}$ values of 53.1 and 62.4 GeV, n varies from a value of ~ 8 at $x_T < 0.2$ to a value of ~ 5 at $x_T \geq 0.3$. A larger value of $n \sim 6.5$ is obtained for $x_T \geq 0.3$, when data at $\sqrt{s} = 30.7$ and 53.1 GeV are used. These results are inconsistent with the scaling law, equation (2), being valid over the entire range of p_T and $\sqrt{s}$ covered by the experiment, either with constant n or with n a function of x_T.

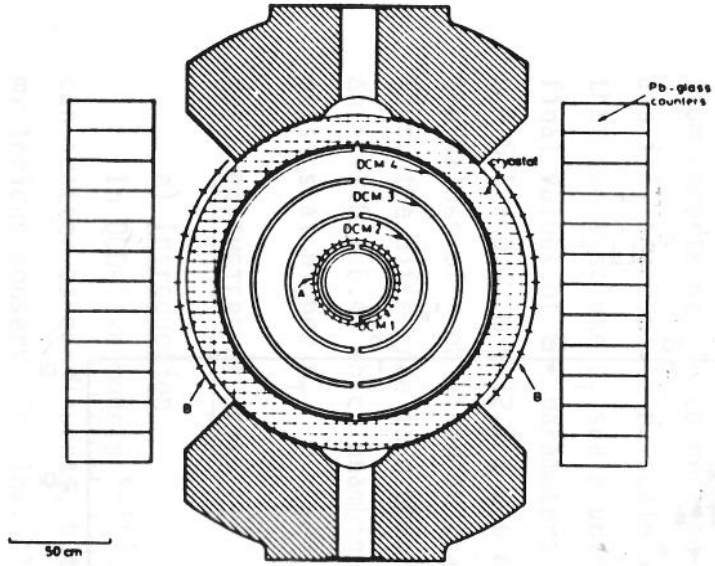
Pb-glass counters
crystal
DCM 4
DCM 3
DCM 2
DCM 1
B
B
50 cm

FIG. 3

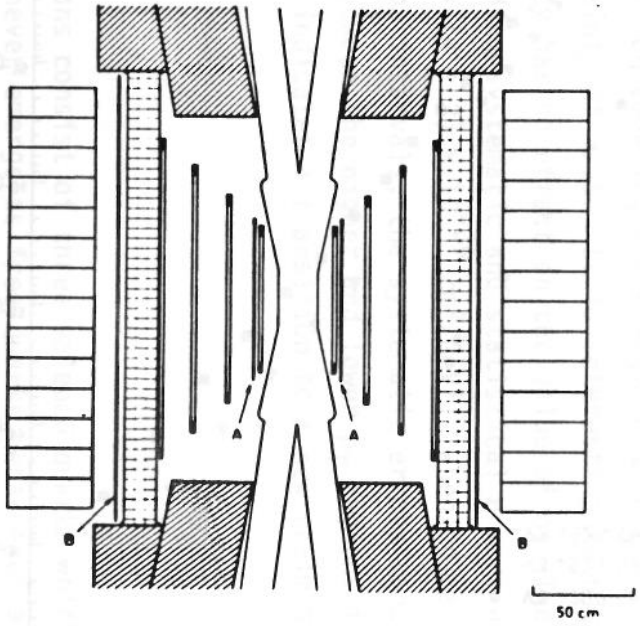
B
B
50 cm

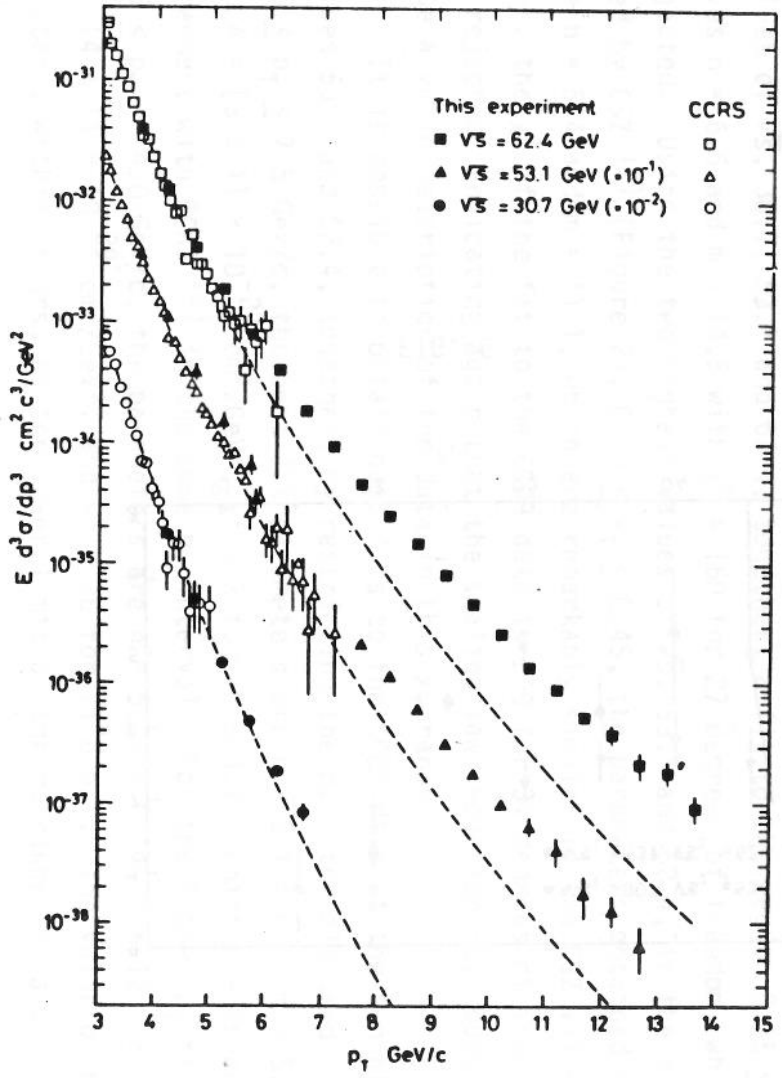
This experiment
CCRS
√s = 62.4 GeV
√s = 53.1 GeV (·10⁻¹)
√s = 30.7 GeV (·10⁻²)
E d³σ/dp³ cm² c³/GeV²
10⁻³¹
10⁻³²
10⁻³³
10⁻³⁴
10⁻³⁵
10⁻³⁶
10⁻³⁷
10⁻³⁸
3 4 5 6 7 8 9 10 11 12 13 14 15
p_T GeV/c

FIG. 4

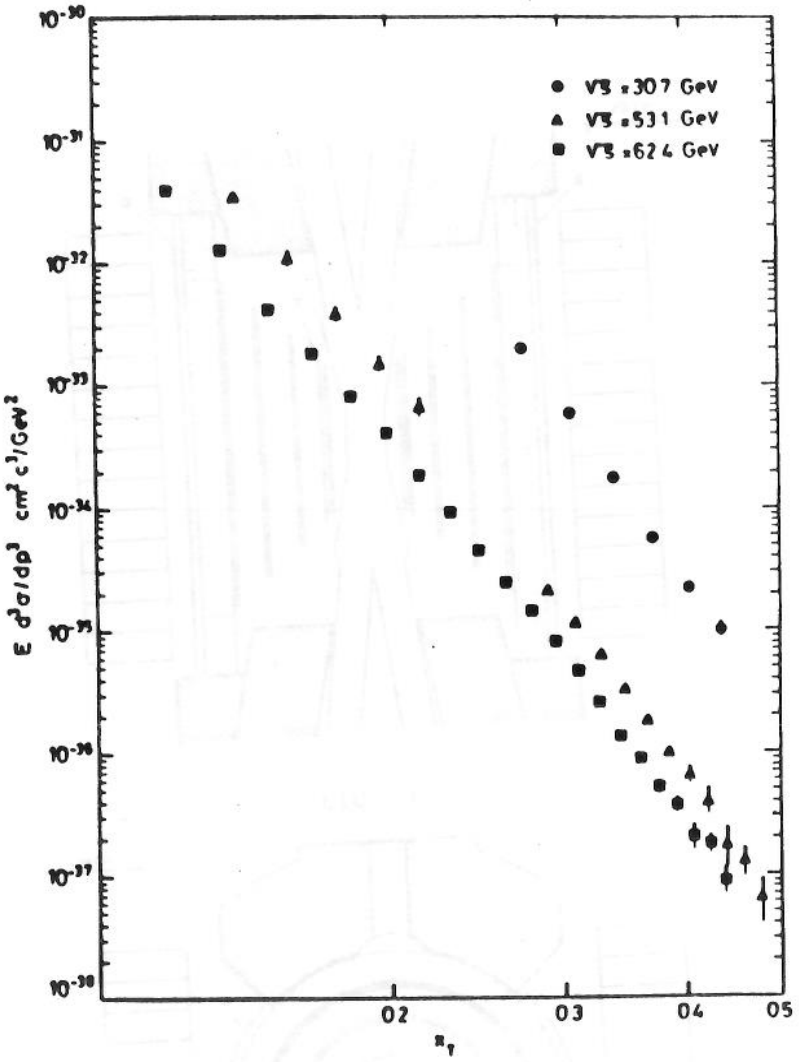
√s = 30.7 GeV
√s = 53.1 GeV
√s = 62.4 GeV
E d³σ/dp³ cm² c³/GeV²
x_T

FIG. 5

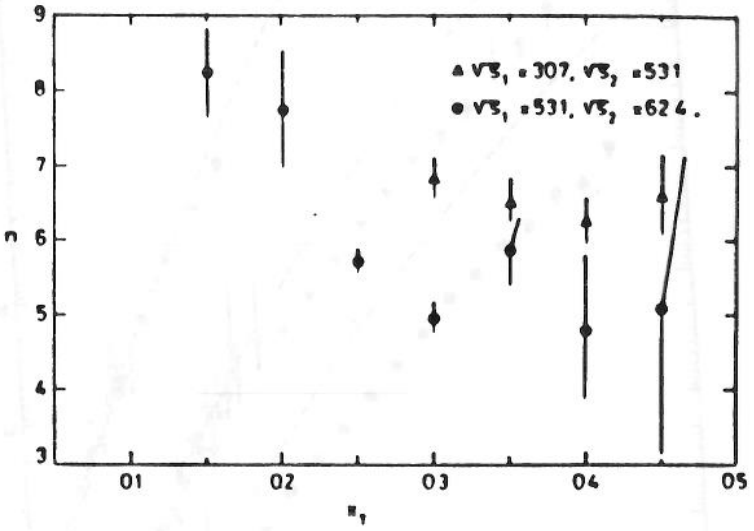
▲ √s₁ = 30.7, √s₂ = 53.1
● √s₁ = 53.1, √s₂ = 62.4.
n
x_T

FIG. 6

The same conclusions can be reached in a more formal way by making fits to the data with the specific scaling form given by equation (6). Using all three values of $\sqrt{s}$, 30.7, 53.1 and 62.4, together, a fit to the region $0.25 \leq x_T \leq 0.5$ gives $n = 6.6$ and $m = 14.5$ with $\chi^2 = 160$ for 27 degrees of freedom, which is rejected. Using the two highest values of $\sqrt{s}$, 53.1 and 62.4, in the x_T region used by CSZ [17] (Figure 2), $0.20 \leq x_T \leq 0.45$, the parameters obtained by CCOR are $n = 6.4$ and $m = 11.1$, which are remarkably similar to the CSZ values. However, the χ^2 of the fit to the CCOR data is 209 for 34 degrees of freedom, which is rejected, indicating again that the scaling law, equation (6), does not provide a valid description of the data in this x_T range.

It is possible to obtain good fits to the CCOR data at the two highest $\sqrt{s}$ values 53.1 and 62.4, together, by restricting the p_T intervals used [22]. For $3.5 \leq p_T \leq 7.5$ GeV/c, the best fit parameters are $n = 8.1 \pm 0.4$, $m = 5.2 \pm 2.1$ and $A = (3 \pm 1) \times 10^{-27}$ cm^2/GeV^2, $\chi^2 = 2$ for 10 d.o.f., which are in adequate agreement with CCRS [18] in the same p_T interval. For the higher p_T range, $7.5 \leq p_T \leq 14.0$ GeV/c, the parameters are $n = 5.06 \pm 0.14$, $m = 12.1 \pm 0.3$, $A = (4 \pm 1) \times 10^{-29}$ cm^2/GeV^2, and $\chi^2 = 26$ for 21 d.o.f. The value of n remains constant, within errors, as the lower limit of the p_T range is raised above 7.5 GeV/c.

The above errors are statistical only. The systematic errors which must be included are: i) a possible ±5% relative normalization error between the data at $\sqrt{s} = 53.1$ and 62.4 GeV; ii) a linear scale error of $\Delta p_T = \pm 0.1$ GeV/c from uncertainty in correcting resolution smearing and energy loss in the coil; and iii) an absolute p_T scale uncertainty of ±5%. It is interesting to note that the absolute p_T scale uncertainty has no effect on the value of n. The final values of the parameters including systematic and statistical errors are $n = 5.1 \pm 0.4$, $m = 12.1 \pm 0.6$ and $A = (4 \pm 2) \times 10^{-29}$ cm^2/GeV^2. When comparing the values of n obtained in the two p_T intervals, the systematic errors cancel. Thus, the difference in n observed between the higher and lower p_T regions is $\Delta n = -3.0 \pm 0.4$, which unambiguously indicates a transition to a new realm of physics at higher p_T.

III - PARAMETERS OF JETS

a) Introduction

In QCD-like models [6-16], protons consist of three valence quarks which can scatter as consituents, but can never emerge as free quarks because of a mysterious conservation law. The scattered quarks are thought to materialize as jets of hadrons at large transverse momenta, while the "spectator" quarks continue in the beam directions, and also rematerialize as jets. A qualitative

prediction of these models is that events at large transverse momenta should consist of two jets which obey the kinematics of elastic scattering in a longitudinally moving center-of-mass frame [23]. Thus the jets should be coplanar with the beam direction and balance transverse momentum. Viewed down the beam axis, in azimuthal projection, the events should show strong azimuthal correlations:

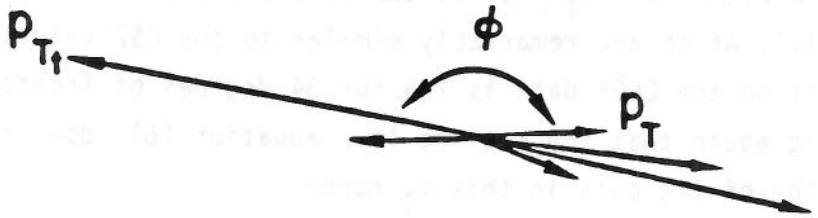

FIG. 7

For experiments with inclusive high p_T triggers, one of the fragments with transverse momentum denoted p_{Tt} or p_{TRIG} will satisfy the trigger.

Independently of any models, the next interesting experimental question is whether there are any other particles associated with a high p_{Tt} inclusive trigger and what their properties are. Given an inclusive trigger on a particle with transverse momentum p_{Tt}, it is easy to measure the conditional probability of observing an associated particle with transverse momentum p_T:

$$P\,(p_T)\Big|_{p_{Tt}}$$

Many experiments this year have produced beautiful data on associated particles which show that the jet picture is believable enough so that the parameters of hadronic jets can be determined. However, the data are not yet good enough to establish or disprove the hypothesis of a di-jet system satisfying quasi-elastic kinematics.

b) Azimuthal Correlations

A case in point is the CCOR experiment [24] (Figure 3). The cylindrical drift chamber system provided full and uniform acceptance over the entire azimuth for charged particles produced in the rapidity range $-0.7 \leq y \leq +0.7$. The apparatus was triggered by either a high p_T π^0, or a minimum bias trigger consisting of a count in any one of the 32 scintillation counters (A) which surrounded the interaction region near DCM1. In both cases a vertex of two or more charged particles was required.

The azimuthal distributions of associated charged particles relative to a π^0 trigger with transverse momentum $p_{Tt} \geq 7.0$ GeV/c are shown in Figure 8 for

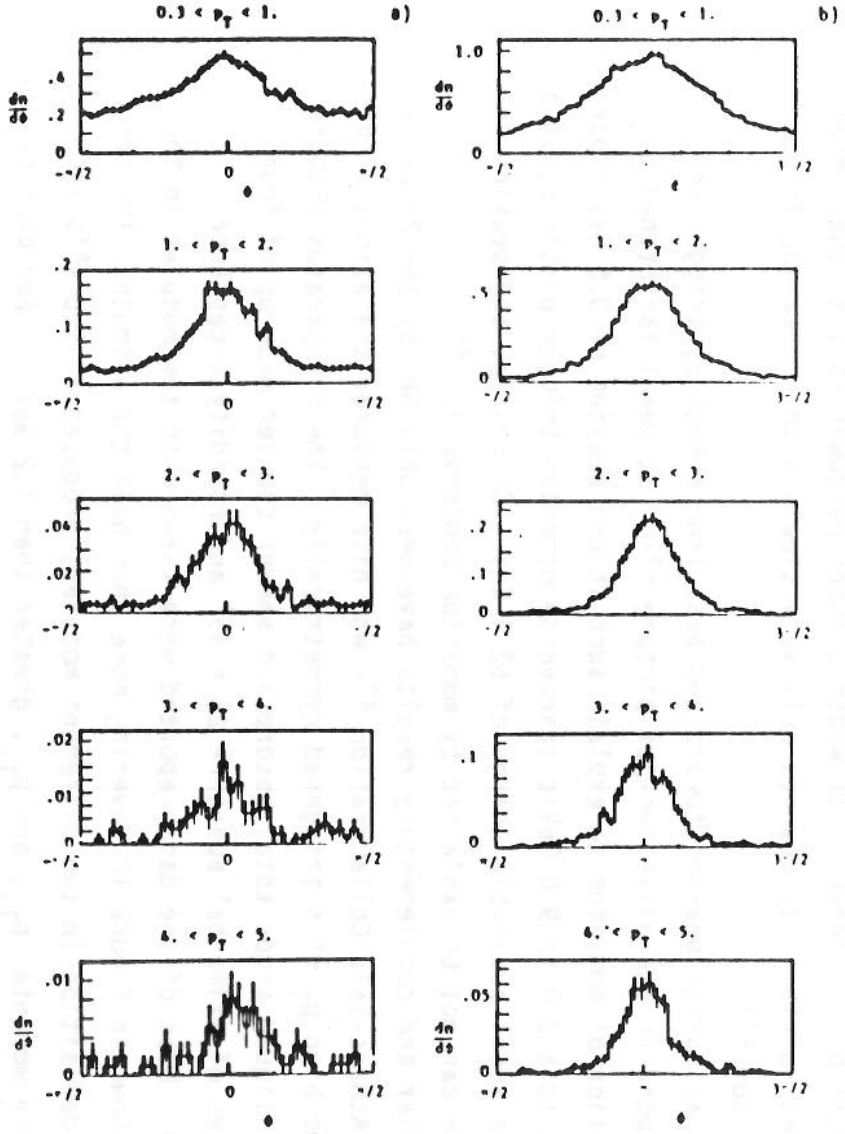
0.3 < p_T < 1. a)
0.3 < p_T < 1. b)
1. < p_T < 2.
1. < p_T < 2.
2. < p_T < 3.
2. < p_T < 3.
3. < p_T < 4.
3. < p_T < 4.
4. < p_T < 5.
4. < p_T < 5.
$\frac{dn}{d\phi}$
ϕ

FIG. 8

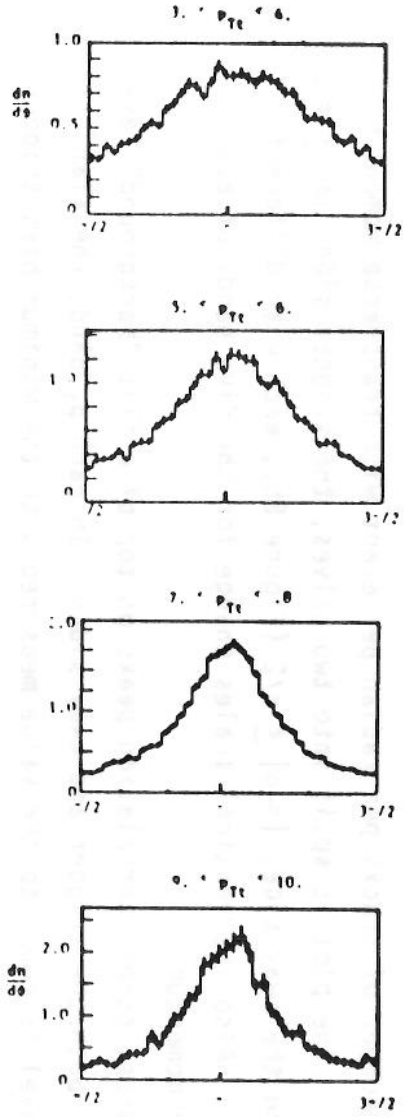
3. < p_{Tt} < 4.
5. < p_{Tt} < 6.
7. < p_{Tt} < 8.
9. < p_{Tt} < 10.
$\frac{dn}{d\phi}$

FIG. 9

five intervals of the associated particle transverse momentum p_T. The quantity plotted

$$\left.\frac{dn(p_T)}{d\phi}\right|_{p_{Tt}}$$

is the average number of tracks per radian per event with transverse momentum $p_{Tt} \geq 7.0$ GeV/c. The plot is split into two halves, the trigger side, $|\phi| \leq \pi/2$ (Figure 8a), and the away side, $|\pi - \phi| \leq \pi/2$ (Figure 8b), each with different vertical scales. Also the vertical scales change for the five bands of associated transverse momentum.

In all cases, strong correlation peaks on top of a flat "background" level are observed on both the trigger and away sides. In each p_T band, the flat "background" level is equal to the value measured with the minimum bias trigger. For associated particle transverse momenta $p_T \geq 1.0$ GeV/c, the flat "background" is negligible in comparison to the two peaks. The widths of both the trigger and away side peaks shrink with increasing associated particle transverse momentum.

It is also informative to look at the away side azimuthal distributions integrated over all associated particle transverse momenta $p_T > 0.30$ GeV/c, as a function of p_{Tt} of the trigger (Figure 9). Compared to the flat "background", which remains constant in all cases, the height of the away peak increases with increasing trigger p_{Tt}. However, its width becomes narrower so that the overall away side charged multiplicity changes only very slowly with increasing trigger transverse momentum [25].

This huge azimuthal peaking toward and away from a high p_T trigger seems to me to correspond to the naive two-jet picture [23]. It seems farfetched to invoke conservation of momentum to explain such strong peaking of 0.5 GeV/c particles relative to a 3.0 to 9.0 GeV/c transverse momentum trigger particle, in a collision with a total available energy of 62.4 GeV. Of course, the peaking on the trigger side can not be explained by momentum conservation [26].

Very similar and complementary results have been obtained by the Brookhaven-CERN-Syracuse-Athens-Yale Collaboration [27] who have measured the azimuthal distribution of two high p_T π^0's triggered symmetrically. Their apparatus (Figure 10) contained a liquid argon total absorption shower counter made up of four identical modules of azimuthal aperture $\Delta\phi = 45^0$ and rapidity acceptance $-0.9 \leq y \leq +0.9$. Most of the data reported were taken with the modules in the configuration shown in Figure 10 covering more than half the azimuth. The trigger was energy deposition in two different modules, produced by two π^0's each having transverse momenta, p_{T_1}, and p_{T_2}, greater than 1.2 GeV/c. For each event,

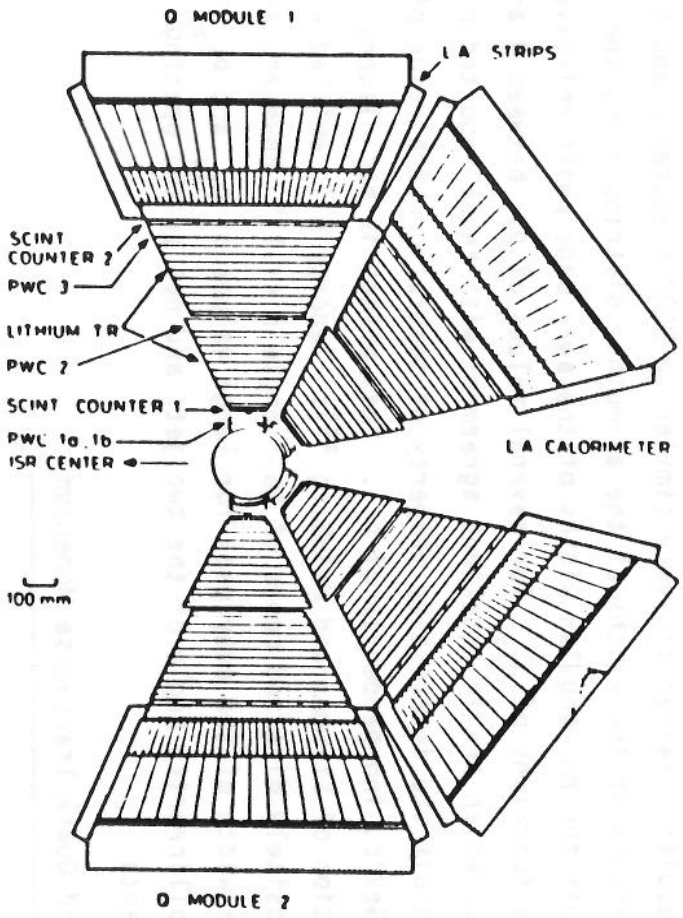
O MODULE 1
LA STRIPS
SCINT COUNTER 2
PWC 3
LITHIUM FR
PWC 2
SCINT COUNTER 1
PWC 1a, 1b
ISR CENTER
LA CALORIMETER
100 mm
O MODULE 2

FIG. 10

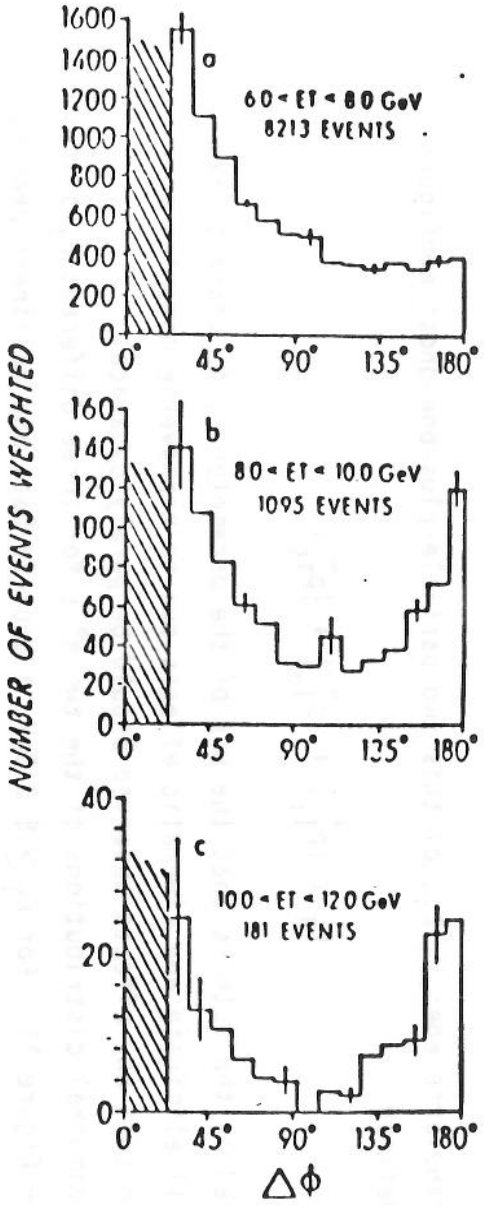
NUMBER OF EVENTS WEIGHTED
a
60 < ET < 80 GeV
8213 EVENTS
b
80 < ET < 100 GeV
1095 EVENTS
c
100 < ET < 120 GeV
181 EVENTS
0°
45°
90°
135°
180°
Δφ

FIG. 11

the transverse momentum p_{Tg} required to balance the vector sum of the transverse momenta of the two observed π^0's was computed,

$$\vec{p}_{Tg} + \vec{p}_{T_1} + \vec{p}_{T_2} \equiv 0 \ .$$

Then the transverse energy, E_T, of this two-particle-plus-one-ghost configuration, was defined

$$E_T \equiv |\vec{p}_{T_1}| + |\vec{p}_{T_2}| + |\vec{p}_{Tg}|$$

It is claimed by the authors that the use of the parameter E_T to characterize the data will eliminate any kinematic effects due to transverse momentum conservation so that any effects observed should be purely dynamical.

The azimuthal distributions of the two π^0's for three different E_T slices are shown in Figure 11. For $E_T \geq 8.0$ GeV, a back-to-back and collinear peaking of the two π^0's is observed. However, for $E_T < 8.0$ GeV the back-to-back peak vanishes. The authors conclude that the two-jet configuration sets in only for $E_T > 8.0$ GeV and that the effect is not due to transverse momentum conservation.

The $E_T \geq 8.0$ GeV condition is always satisfied when one of the two triggering π^0's has transverse momentum $p_{T_1} \geq 4$ GeV/c. Thus, calling p_{T_1} the larger transverse momentum of the two π^0's and p_{T_2} the smaller, the authors also show azimuthal distributions of the two π^0's in slices of "associated" transverse momentum p_{T_2} for various values of the "trigger" transverse momentum p_{T_1} (Figure 12). The results obtained are very similar to CCOR (Figures 8 and 9). Making a further analysis of the widths of the azimuthal distributions, the BCSAY group also plots the rms angular widths of the away side peaks relative to the "trigger", as functions of p_{T_2}, for several values of p_{T_1} between 4 and 9 GeV/c. The widths, which are in excellent agreement with those reported by CCOR [1], seem to exhibit the interesting property of saturation at a value of $\sim 13^0$, for $p_{T_2} > 3$ GeV/c, independently of p_{T_1}. This effect is reminiscent of the QCD jet description of Sterman and Weinberg [28]: "energy E is emitted within some pair of oppositely directed cones of half angle $\delta << 1$." However, as we shall see later, the width of the away peak for large values of p_{T_1} and p_{T_2} is dominated by the acollinearity angle of the two jets and not by the opening angles of the fragments.

c) p_{out}, x_E and Quark Transverse Momentum

In order to get some additional quantitative information from the azimuthal distributions, historically [29] two variables, p_{out} and x_E, were defined

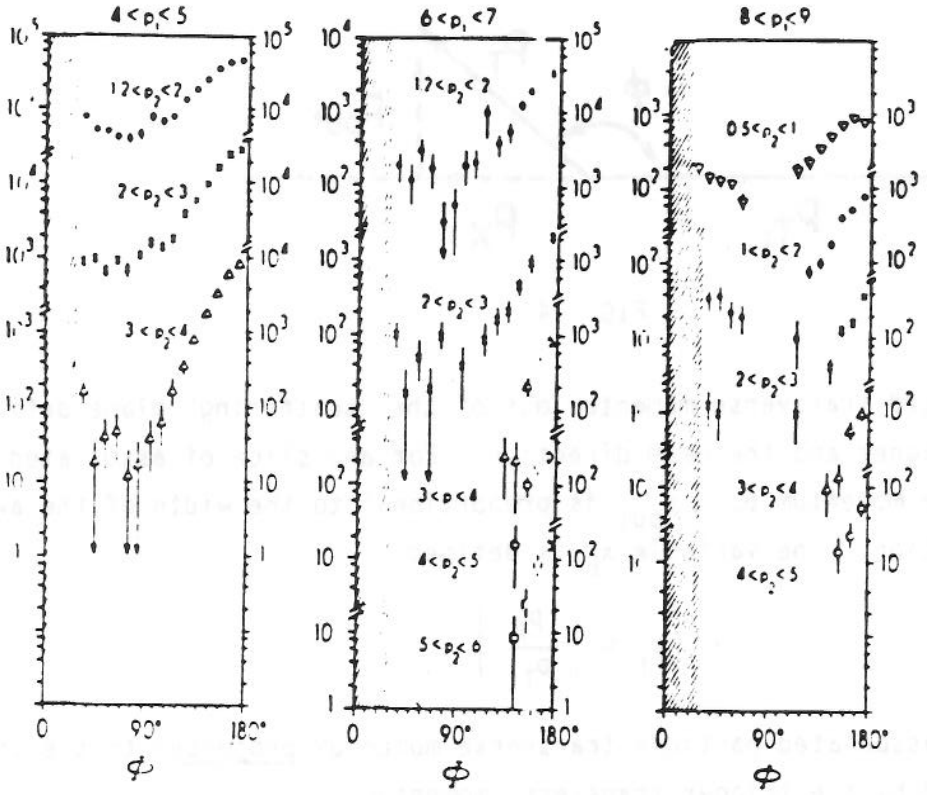
4 < p1 < 5
6 < p1 < 7
8 < p1 < 9
1.2 < p2 < 2
2 < p2 < 3
3 < p2 < 4
4 < p2 < 5
5 < p2 < 6
0.5 < p2 < 1
1 < p2 < 2
0
90°
180°
Φ

FIG. 12

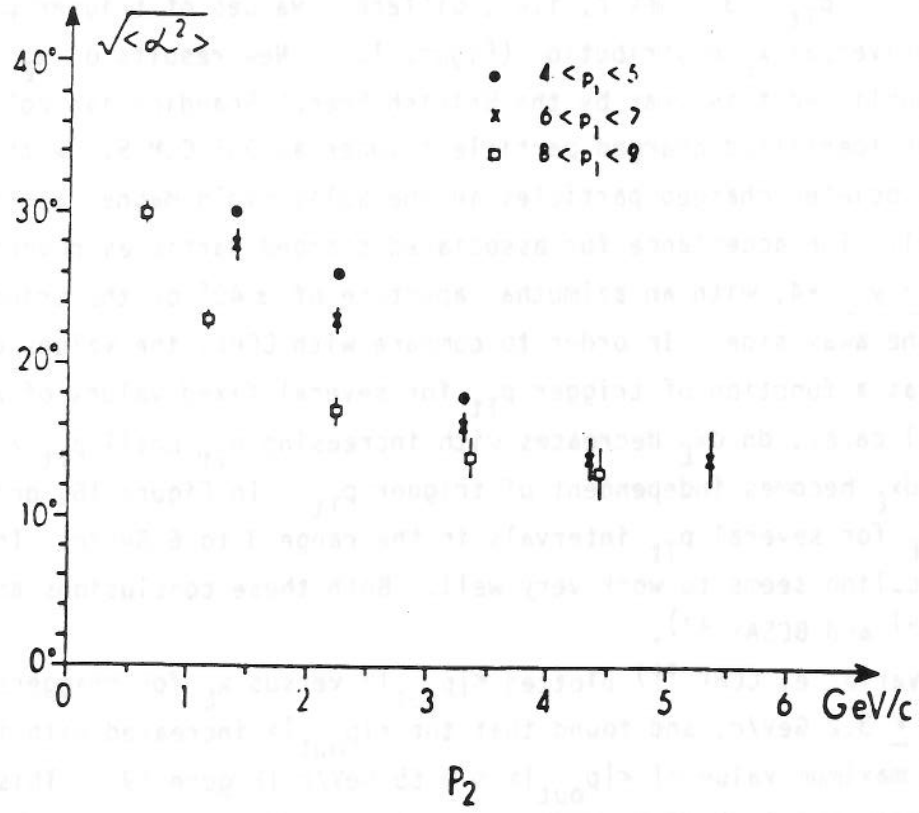
√<α²>
40°
30°
20°
10°
0°
0
1
2
3
4
5
6 GeV/c
P2
4 < p1 < 5
6 < p1 < 7
8 < p1 < 9

FIG. 13

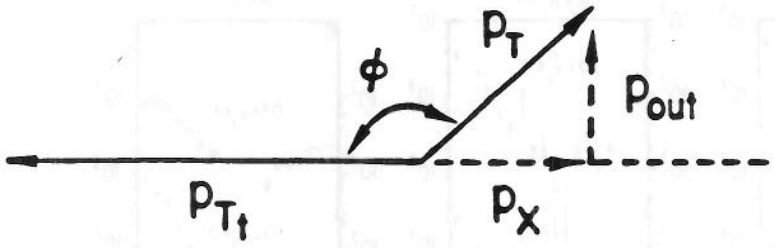

FIG. 14

p_{out} is the projected transverse momentum out of the "scattering" plane defined by the high p_{Tt} trigger and the beam direction. For any slice of associated particle transverse momentum p_T , p_{out} is proportional to the width of the away azimuthal distribution. The variable x_E is defined

$$x_E = \left| \frac{p_x}{p_{Tt}} \right|$$

so that x_E is the associated particle transverse momentum <u>projected</u> to the trigger axis and <u>scaled</u> by the trigger transverse momentum.

Historically (in 1977) it was found by the CERN-College de France-Heidelberg-Karlsruhe Group [30] working at the ISR that x_E scaling [31] didn't work in the range $2.0 \leq p_{Tt} \leq 3.2$ GeV/c; i.e., different values of trigger p_{Tt} did not produce a universal x_E distribution (Figure 15). New results on x_E scaling have been published this year by the British-French-Scandinavian collaboration [32] using an identified charged particle trigger at 90° C.M.S., with detection of the associated charged particles in the Split Field Magnet at the CERN ISR (Figure 17). The acceptance for associated charged particles covers a rapidity range $-4 \leq y \leq +4$, with an azimuthal aperture of $\pm 40^0$ on the trigger side and $\pm 25^0$ on the away side. In order to compare with CCHK, the values of dn/dx_E are plotted as a function of trigger p_{Tt} for several fixed values of x_E (Figure 18). In all cases, dn/dx_E decreases with increasing p_{Tt} until $p_{Tt} > 3$ GeV/c whereupon dn/dx_E becomes independent of trigger p_{Tt}. In Figure 16, dn/dx_E is plotted versus x_E for several p_{Tt} intervals in the range 3 to 6 GeV/c. In this p_T range, x_E scaling seems to work very well. Both these conclusions are confirmed by CCOR [24] and BCSAY [27].

For the p_{out} variable, CCHK [30] plotted $\langle|p_{out}|\rangle$ versus x_E for triggers in the range $2.0 \leq p_{Tt} \leq 3.2$ GeV/c, and found that the $\langle|p_{out}|\rangle$ increased with increasing x_E up to a maximum value of $\langle|p_{out}|\rangle \sim 0.65$ GeV/c (Figure 19). This effect [33] coupled with the lack of x_E scaling for $p_{Tt} < 3$ GeV/c was taken by CCHK as evidence for the transverse momentum of quarks inside the proton [34]. Do the new results this year change this picture?

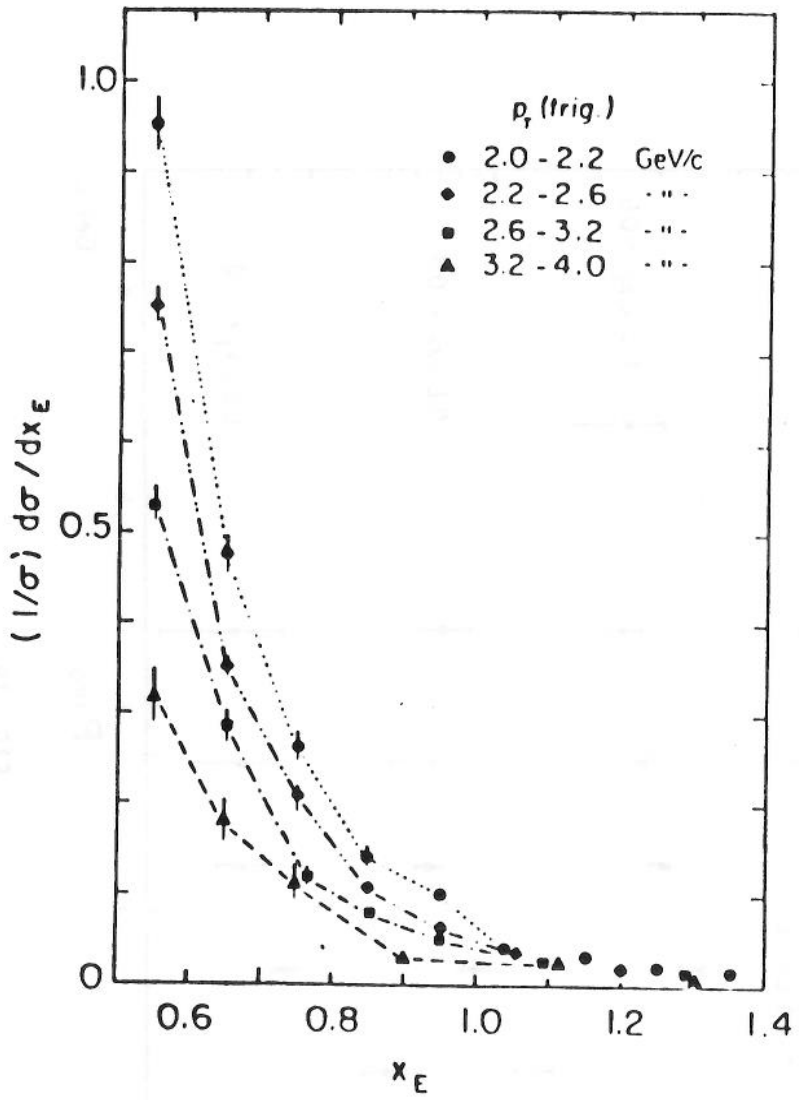
p_T (trig.)
2.0 - 2.2 GeV/c
2.2 - 2.6 - " -
2.6 - 3.2 - " -
3.2 - 4.0 - " -
$(1/\sigma)\, d\sigma/dx_E$
1.0
0.5
0
0.6
0.8
1.0
1.2
1.4
x_E

FIG. 15

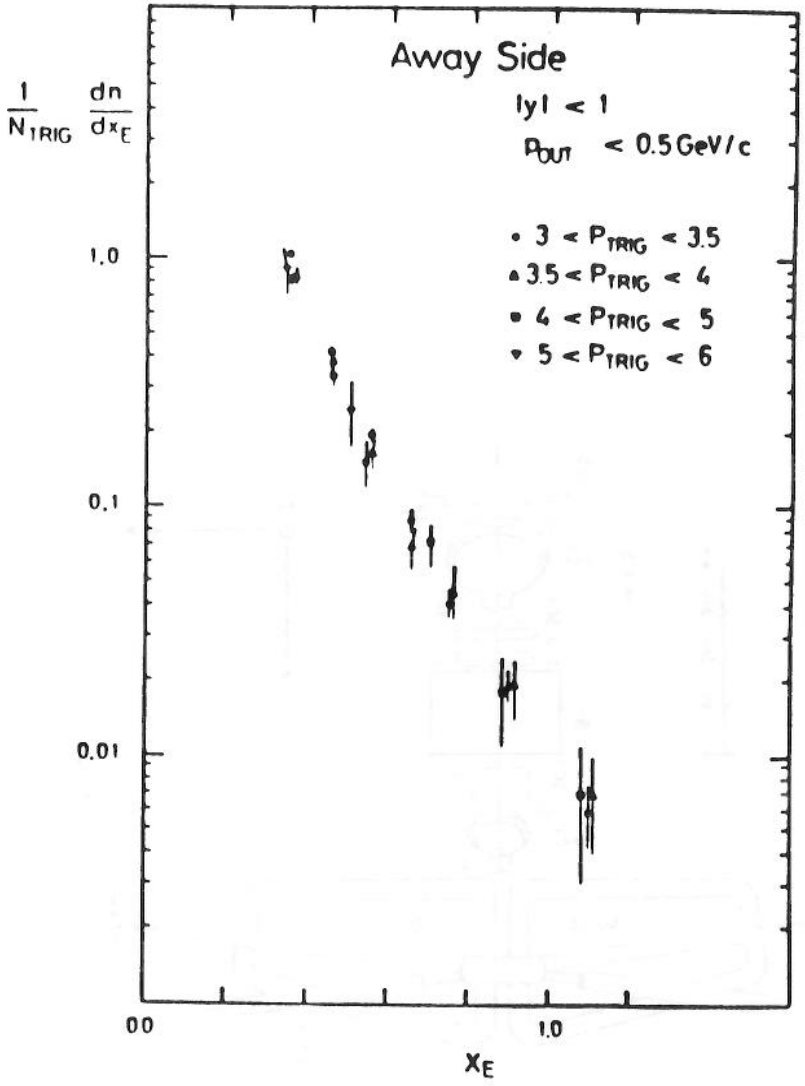
Away Side
$\frac{1}{N_{TRIG}} \frac{dn}{dx_E}$
|y| < 1
P_{OUT} < 0.5 GeV/c
• 3 < P_{TRIG} < 3.5
▲ 3.5 < P_{TRIG} < 4
■ 4 < P_{TRIG} < 5
▼ 5 < P_{TRIG} < 6
1.0
0.1
0.01
00
1.0
x_E

FIG. 16

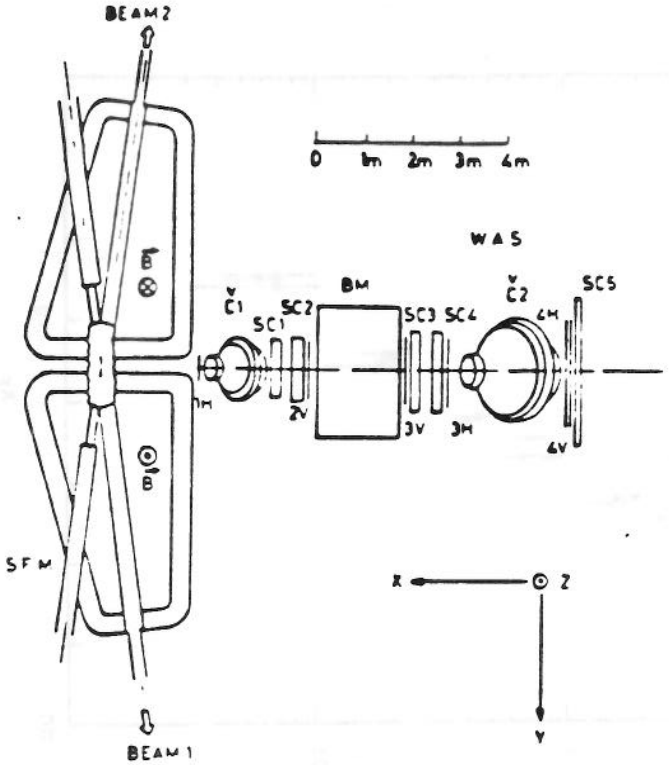
BEAM 2
0 1m 2m 3m 4m
WAS
B
C1
SC1
SC2
BM
SC3
SC4
C2
SC5
1H
2V
3V
3H
4H
4V
B
SFM
x
z
y
BEAM 1

FIG. 17

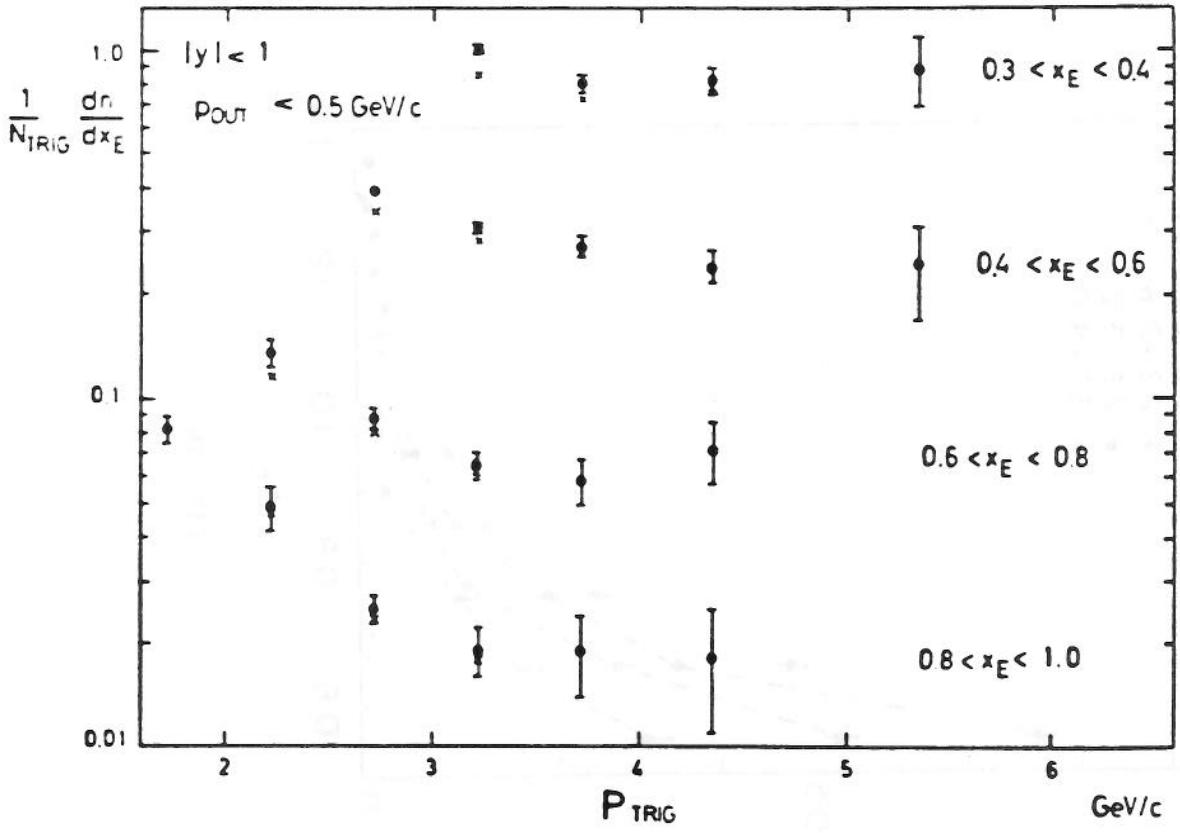
1.0
0.1
0.01
|y| < 1
p_{OUT} < 0.5 GeV/c
$\frac{1}{N_{TRIG}} \frac{dn}{dx_E}$
0.3 < x_E < 0.4
0.4 < x_E < 0.6
0.6 < x_E < 0.8
0.8 < x_E < 1.0
2
3
4
5
6
P_{TRIG}
GeV/c

FIG. 18

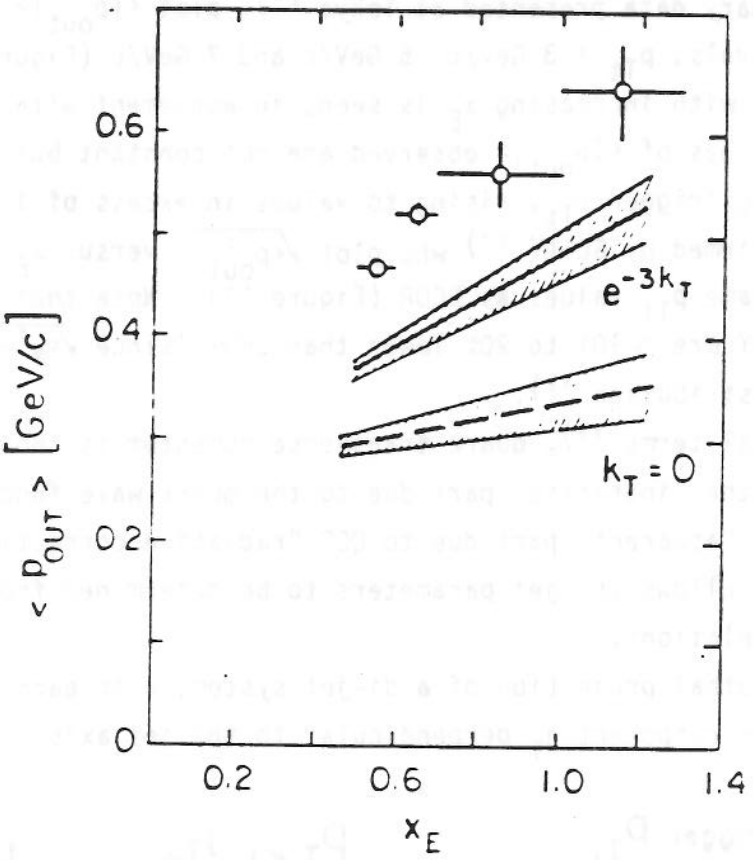
0.6
0.4
0.2
0
0.2
0.6
1.0
1.4
x_E
$< p_{OUT} > [GeV/c]$
e^{-3k_T}
$k_T = 0$

FIG. 19

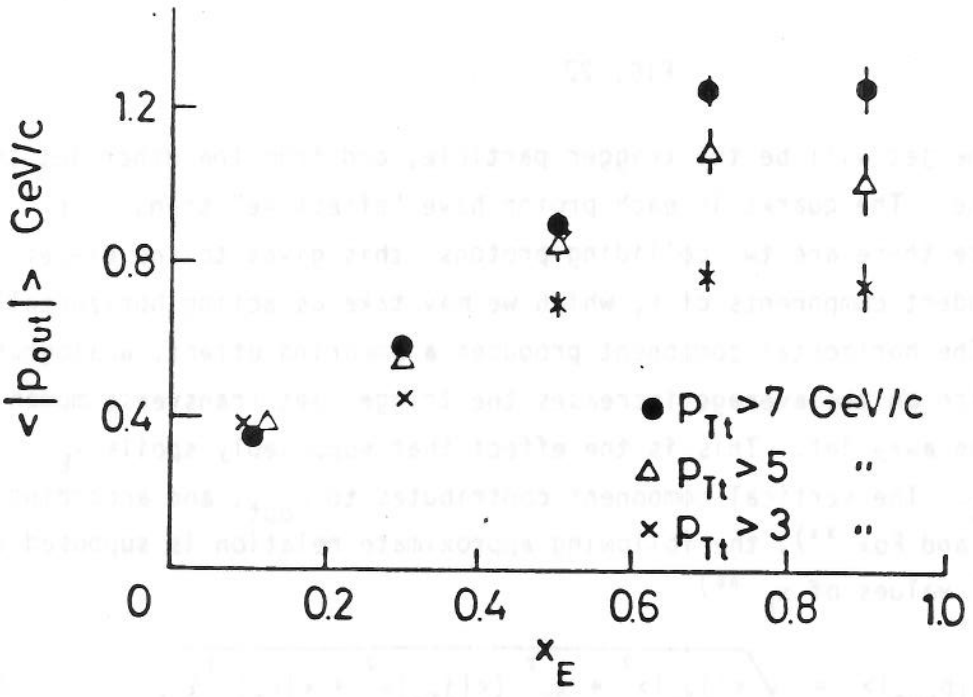
1.2
0.8
0.4
0
0.2
0.4
0.6
0.8
1.0
x_E
$<|p_{out}|>$ GeV/c
$p_{Tt}>7$ GeV/c
$p_{Tt}>5$ "
$p_{Tt}>3$ "

FIG. 20

CCOR, in preliminary data presented at Tokyo [24], plot $<|p_{out}|>$ versus x_E for three trigger intervals, $p_{Tt} > 3$ GeV/c, 5 GeV/c and 7 GeV/c (Figure 20). An increase of $<|p_{out}|>$ with increasing x_E is seen, in agreement with CCHK. However, the maximum values of $<|p_{out}|>$ observed are not constant but tend to increase with increasing trigger p_{Tt}, rising to values in excess of 1.0 GeV/c. This same trend is confirmed by BCSAY [27] who plot $\sqrt{<p_{out}^2>}$ versus x_E (which they call z), for the same p_{Tt} values as CCOR (Figure 21). Note that the $<|p_{out}|>$ values of BCSAY are $\sim$10% to 20% lower than CCOR (since $\sqrt{<y^2>} = \sqrt{\pi/2} \times <|y|>$ for a Gaussian distribution [35]).

In phenomenological terms [33], quark transverse momentum is thought to be composed of two parts, the "intrinsic" part due to the quark wave function inside the proton and the "apparent" part due to QCD "radiative corrections". This same phenomenology allows the jet parameters to be determined from the two-particle azimuthal correlations.

Consider the azimuthal projection of a di-jet system, with each jet having a fragment with momentum component j_T perpendicular to the jet axis.

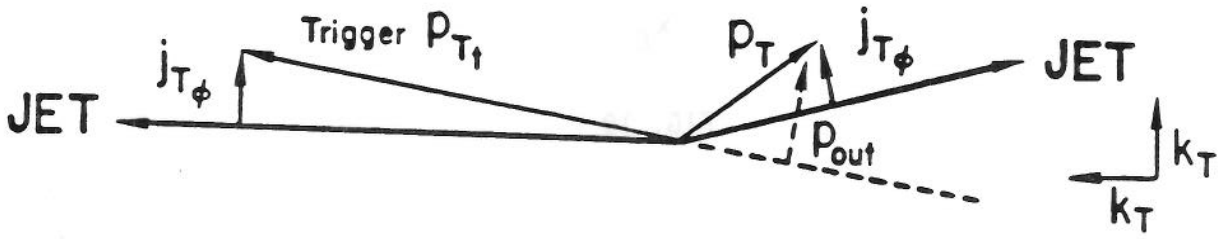

FIG. 22

A fragment from one jet will be the trigger particle, and from the other jet the associated particle. The quarks in each proton have "effective" transverse momentum k_T. Since there are two colliding protons, this gives to the di-jet system two independent components of k_T which we may take as acting horizontally and vertically. The horizontal component produces a smearing effect, analogous to resolution, which on the average increases the trigger jet transverse momentum relative to the away jet. This is the effect that supposedly spoils x_E scaling at low p_{Tt}. The vertical component contributes to p_{out}, and according to Feynman, Field and Fox [33], the following approximate relation is supposed to be valid for small values of x_E [36] :

$$<|p_{out}|> = \sqrt{<|j_{T\phi}|>^2 + x_E^2 \left(<|j_{T\phi}|>^2 + <|k_T|>^2\right)} \quad . \qquad (7)$$

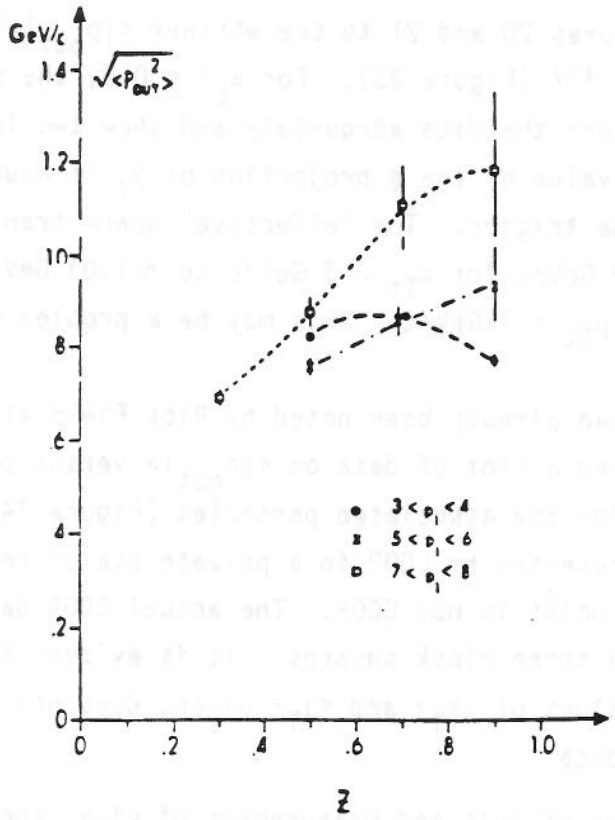

FIG. 21

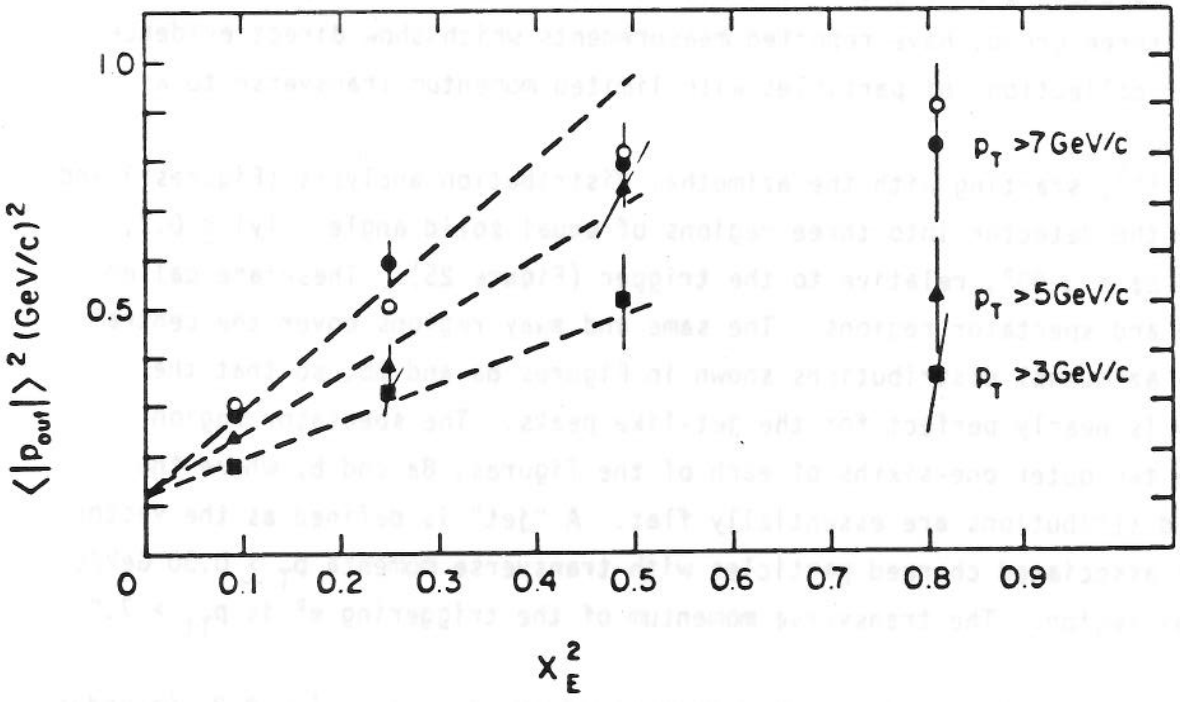

FIG. 23. $\langle |p_{out}| \rangle^2$ versus x_E^2 : Solid points CCOR data [37]; open circles BCSAY data from Figure 21.

I have replotted Figures 20 and 21 to see whether $<|p_{out}|>^2$ versus x_E^2 is a reasonable straight line [37] (Figure 23). For $x_E^2 \leq 0.5$, the straight lines illustrated seem to represent the data adequately and show two interesting features. The mean absolute value of the ϕ projection of j_T is equal to 0.35 GeV/c independently of p_{Tt} of the trigger. The "effective" quark transverse momentum, $<k_T>$ increases from $\sim$0.78 GeV/c for $p_{Tt} > 3$ GeV/c to $\sim$1.03 GeV/c for $p_{Tt} > 5$ GeV/c to $\sim$1.25 GeV/c for $p_{Tt} > 7$ GeV/c. This may be a problem or, rather, a challenge for QCD.

This latter effect had already been noted by Rick Field at the Copenhagen Jet Symposium[38]. He showed a plot of data on $<|p_{out}|>$ versus p_{Tt}, with the condition $p_T > 1.0$ GeV/c for the associated particles (Figure 24). The data say "CCOR", and were indeed presented by CCOR in a private status report [39]. However, the lowest p_{Tt} data point is not CCOR. The actual CCOR data [24,37] are shown on the figure by the three black squares. It is evident that the curve labeled "QCD", with the values of $<k_T>$ and $<j_T>$ given, does not provide an adequate description of the data.

d) Direct Observation of Jets and Measurement of $<j_T>$, the Mean Momentum Transverse to the Jet Axis

The variation of $<|p_{out}|>$ with x_E is a simple and elegant way of determining the parameters of a jet model; but it doesn't prove that jets exist! This year, three groups have reported measurements which show direct evidence for jets as collections of particles with limited momentum transverse to a common axis.

CCOR [24], starting with the azimuthal distribution analysis (Figures 3 and 8), divide the detector into three regions of equal solid angle: $|y| \leq 0.7$, fixed, and $\Delta\phi = \pm 60^0$, relative to the trigger (Figure 25). These are called away, same and spectator regions. The same and away regions cover the central 2/3 of the azimuthal distributions shown in Figures 8a and 8b, so that the acceptance is nearly perfect for the jet-like peaks. The spectator region covers the two outer one-sixths of each of the figures, 8a and b, where the azimuthal distributions are essentially flat. A "jet" is defined as the vector sum of all associated charged particles with transverse momenta $p_T \geq 0.30$ GeV/c in the away region. The transverse momentum of the triggering π^0 is $p_{Tt} > 7.0$ GeV/c.

A centering cut is made on the rapidity of the jet, $|y_{jet}| \leq 0.3$, in order to eliminate edge effects. Then the mean projected momentum of fragments transverse to the sum vector is taken on two orthogonal axes, one of which lies in the azimuthal plane. These two projections, $<|j_{T\theta}|>$ and $<|j_{T\phi}|>$, are plotted in Figure 26 as a function of p_T of the jet fragment, for all jets with $|\Sigma \vec{p}_T| >$

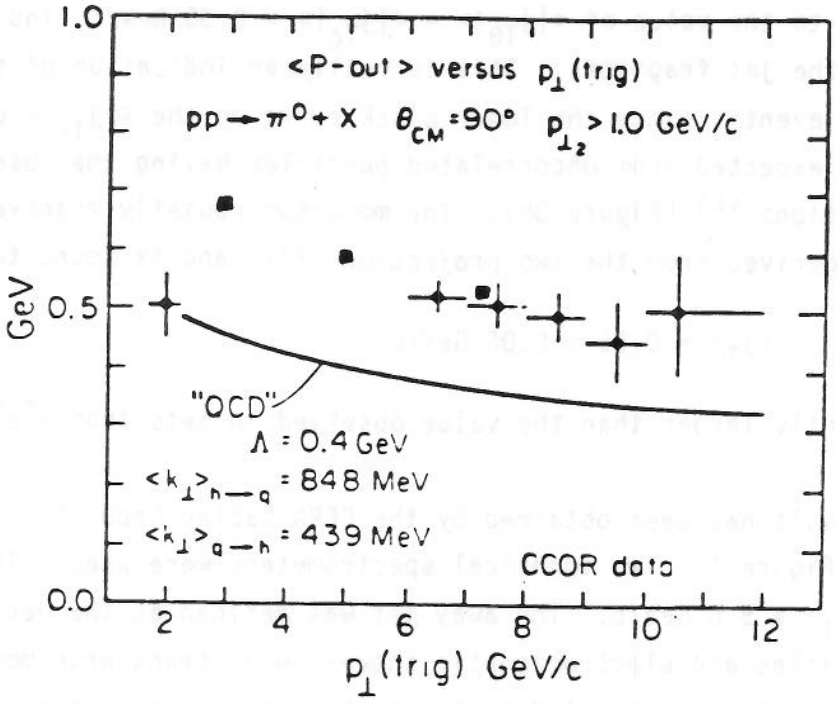
<P-out> versus $p_\perp$(trig)
$pp \to \pi^0 + X$ $\theta_{CM}=90°$ $p_{\perp_2} > 1.0$ GeV/c
GeV
1.0
0.5
0.0
"QCD"
$\Lambda = 0.4$ GeV
$\langle k_\perp \rangle_{h-q} = 848$ MeV
$\langle k_\perp \rangle_{q-h} = 439$ MeV
CCOR data
2
4
6
8
10
12
$p_\perp$(trig) GeV/c

FIG. 24

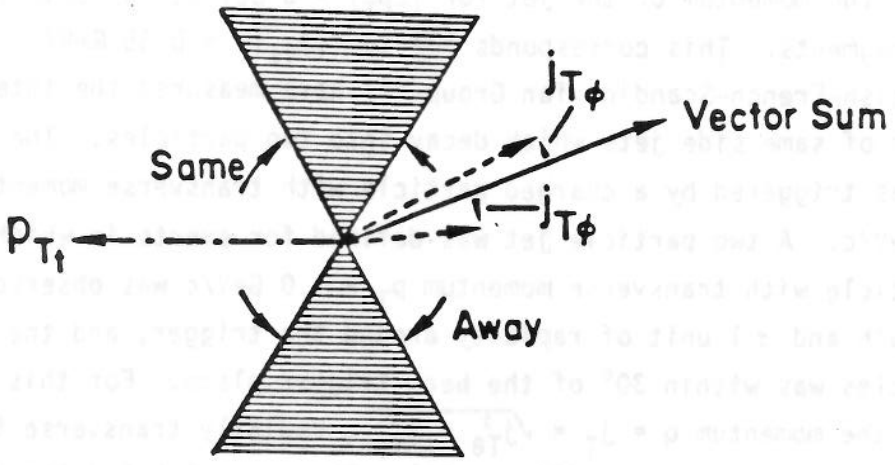
$j_{T\phi}$
Vector Sum
Same
p_{T_t}
$j_{T\phi}$
Away

FIG. 25

3 GeV/c. The two projected mean transverse momenta are observed to be equal to each other, and limited to the value of $\langle|j_{T\theta}|\rangle = \langle|j_{T\phi}|\rangle = 0.35$ GeV/c, independently of the p_T of the jet fragments. This is really an indication of the jettiness of individual events, since the lower black curve on the $\langle|j_{T\phi}|\rangle$ plot indicates what would be expected from uncorrelated particles having the observed away azimuthal distributions [40] (Figure 8b). The momentum radially transverse to the jet axis can be derived from the two projections [35], and is found to be

$$\langle j_T \rangle = 0.55 \pm 0.06 \text{ GeV/c} .$$

This value is significantly larger than the value observed in jets from e^+e^- collisions [41].

A very similar result has been obtained by the CERN-Saclay Group [42] using the apparatus shown in Figure 1. Two identical spectrometers were used. The trigger was a π^0 with $p_{Tt} > 5.0$ GeV/c. The away jet was defined as the vector sum of all charged particles and electromagnetic showers with transverse momenta $p_T > 0.80$ GeV/c, observed within the solid angle of the away spectrometer. Since the acceptance of the spectrometer was rather limited, particularly in ϕ ($\Delta\phi = \pm 15^0$), it was necessary to use a Monte Carlo program to interpret the experimental results. The observed projected distributions in $j_{T\theta}$ for both the charged and neutral fragments of jets with $|\Sigma \vec{p}_T| > 3.0$ GeV/c are shown in Figure 27, together with Monte Carlo predictions for $\sqrt{\langle j_{T\theta}^2 \rangle} = 0.30$, 0.45 and 0.60 GeV/c. The data are consistent with a constant value of

$$\sqrt{\langle j_{T\theta}^2 \rangle} = 0.44 \pm 0.04 \text{ GeV/c} ,$$

independent of the momentum of the jet for $|\Sigma \vec{p}_T| > 3$ GeV/c, for both the charged and neutral fragments. This corresponds [35] to $\langle|j_{T\theta}|\rangle = 0.35$ GeV/c.

The British-French-Scandinavian Group [32] have measured the internal transverse momentum of same side jets which decay into two particles. The apparatus (Figure 16) was triggered by a charged particle with transverse momentum $p_{TRIG} > 2.5$ GeV/c. A two particle jet was defined for events in which one other same side particle with transverse momentum $p_T > 1.0$ GeV/c was observed within $\pm 35^0$ in azimuth and ± 1 unit of rapidity around the trigger, and the plane of the two particles was within 30^0 of the beam-trigger plane. For this two particle system, the momentum $q = j_T = \sqrt{j_{T\theta}^2 + j_{T\phi}^2}$, radially transverse to the vector sum axis was histogrammed (Figure 28). The curve labeled "background" was obtained by superimposing a typical trigger spectrum with $p_{TRIG} > 2.5$ GeV/c on a sample of minimum bias events. A clear effect is observed in the difference between the data and the background, which corresponds to

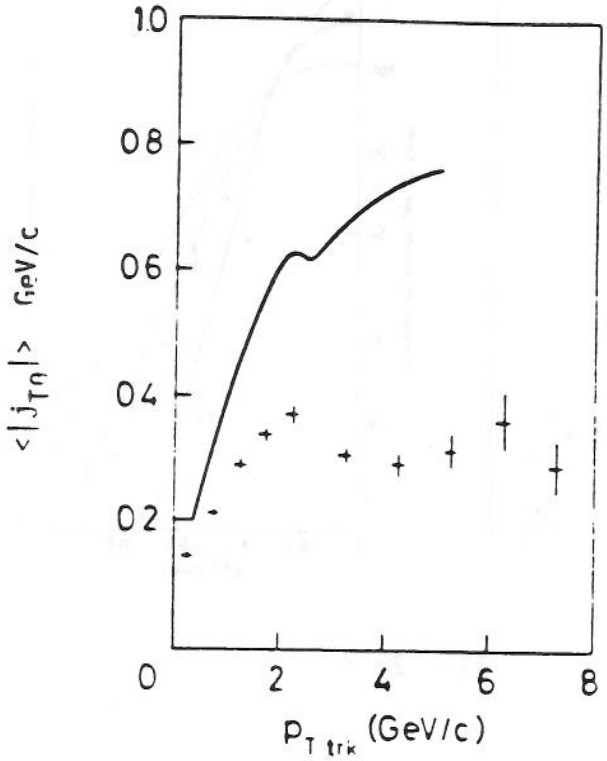
1.0
0.8
0.6
0.4
0.2
0
2
4
6
8
$<|j_{T\eta}|>$ GeV/c
$p_{T\,trk}$ (GeV/c)

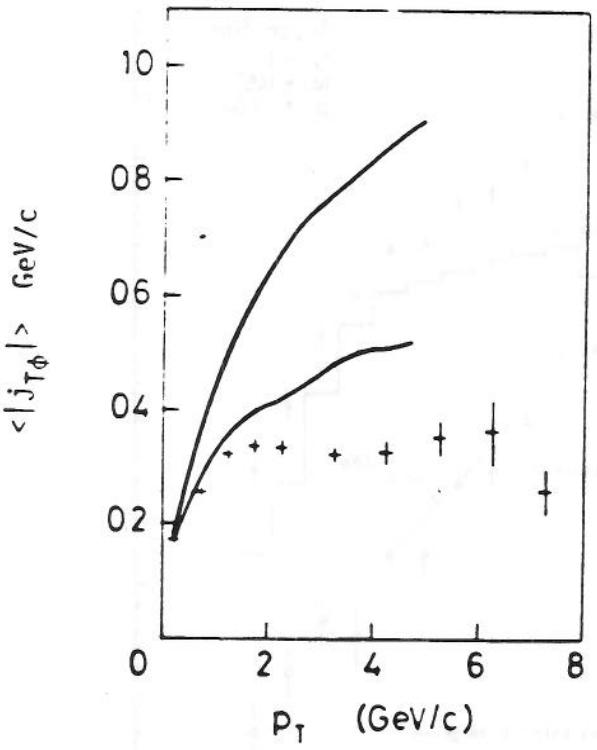
10
0.8
0.6
0.4
0.2
0
2
4
6
8
$<|j_{T\phi}|>$ GeV/c
p_T (GeV/c)

FIG. 26

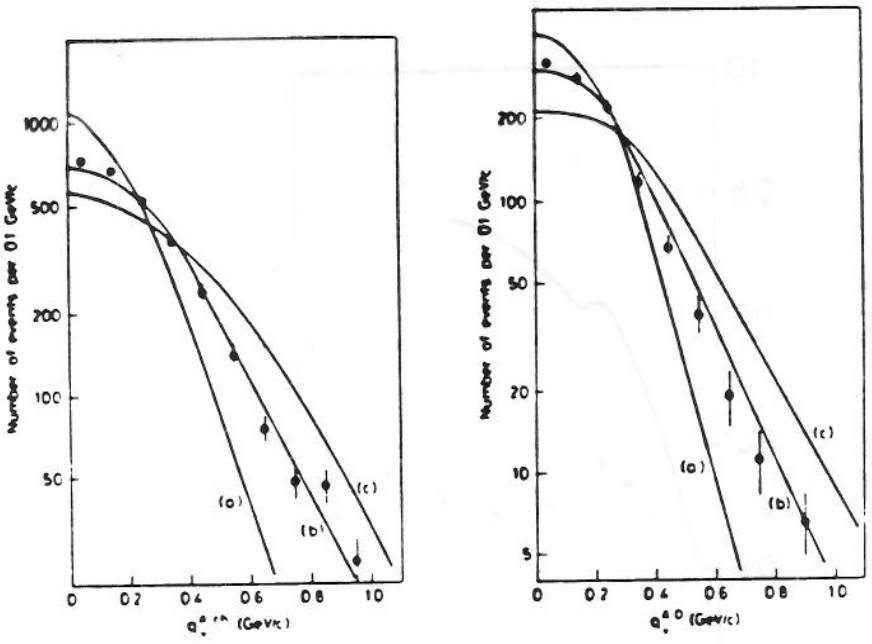
1000
500
200
100
50
0
0.2
0.4
0.6
0.8
1.0
(a)
(b)
(c)
200
100
50
20
10
5

FIG. 27

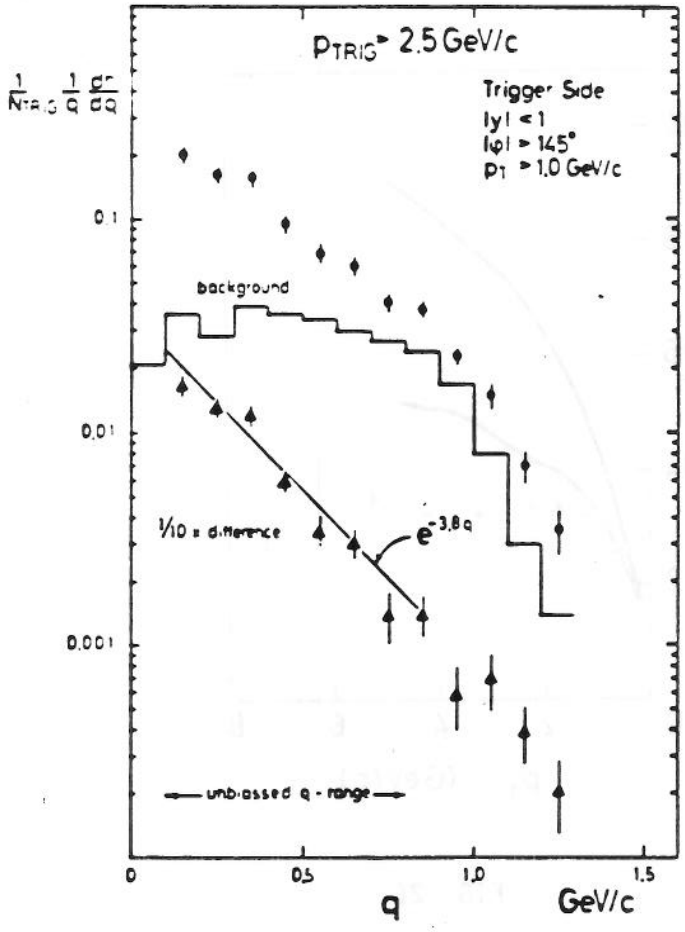
$p_{TRIG} > 2.5$ GeV/c
Trigger Side
$|y| < 1$
$|\varphi| > 145°$
$p_T > 1.0$ GeV/c
background
1/10 x difference
$e^{-3.8q}$
unbiassed q - range
0.1
0.01
0.001
0
0.5
1.0
1.5
q
GeV/c

FIG. 28

$$\langle j_T \rangle = 0.52 \pm 0.05 \text{ GeV/c}$$

Except for minor technicalities, all three experiments are consistent with symmetric fragmentation about the jet axis with constant average transverse momentum [41]

$$\langle j_T \rangle = 0.55 \text{ GeV/c}$$

or $$\sqrt{\langle j_T^2 \rangle} = 0.62 \text{ GeV/c}$$ to within $\sim 10\%$.

e) Transverse Momentum Balance of Jets

Although the jettiness of the events is clearly established, there has been no proof given by any of these experiments that the high p_T reaction consists of a system of two jets, roughly balancing transverse momentum, and satisfying quasi-elastic kinematics [43]. CCOR, so far, has only used charged particles in the away jet, so that no transverse momentum balance would be expected. However, the sum of x_E for all charged particles in the away region was studied. The distributions in $\Sigma\, x_E^a$ for different values of trigger p_{Tt} (Figure 29) exhibit scaling, i.e., they don't depend on p_{Tt}.

CERN-Saclay [42] made a more serious attempt at studying the transverse momentum balance of jets by reconstructing both the same and away side jets from all charged particles and electromagnetic showers with $p_T > 0.80$ GeV/c observed in their two spectrometer system. However, since the solid angle of this system was limited, and because the $p_T > 0.80$ GeV/c cut had a considerable effect, it was again necessary to resort to a jet Monte Carlo calculation in order to interpret the results. A plot of the number of events as a function of their observed transverse momentum balance B is shown in Figure 30, where B is defined as

$$B \equiv \left|\Sigma\, \vec{p}_T\right|_{\text{away}} \Big/ \left|\Sigma\, \vec{p}_T\right|_{\text{same}} .$$

The data points show no indication of momentum balance. The black curves represent jet Monte Carlo calculations with various assumptions about the rapidity and azimuthal correlations of the pair of jets. The curve best fitting the data corresponds to an away jet which balances only 80% of the trigger jet transverse momentum, even after correction for k_T smearing. For my taste, there is nothing at all compelling about this conclusion, since it is not readily apparent from the data but is completely dependent on the assumptions of the Monte Carlo jet program. What is needed in this field is an experiment with considerably larger acceptance, particularly in azimuth.

f) Fragmentation Distributions of Trigger Side Jets

It is important to stress that the naive two jet model has been neither proved nor disproved by any of the results presented so far. Furthermore, all

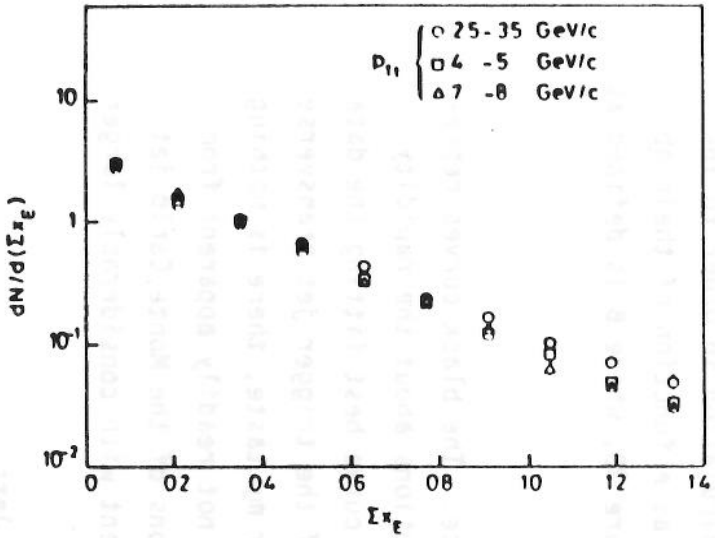

FIG. 29

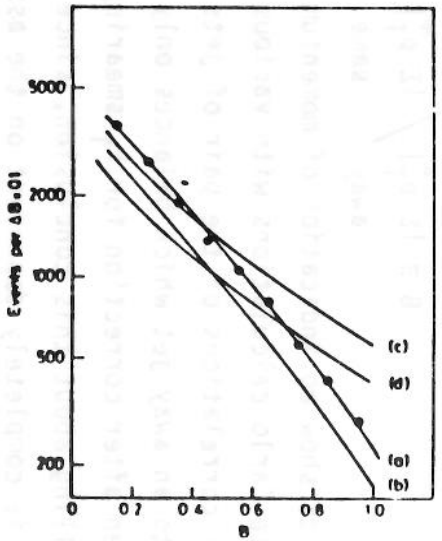

FIG. 30

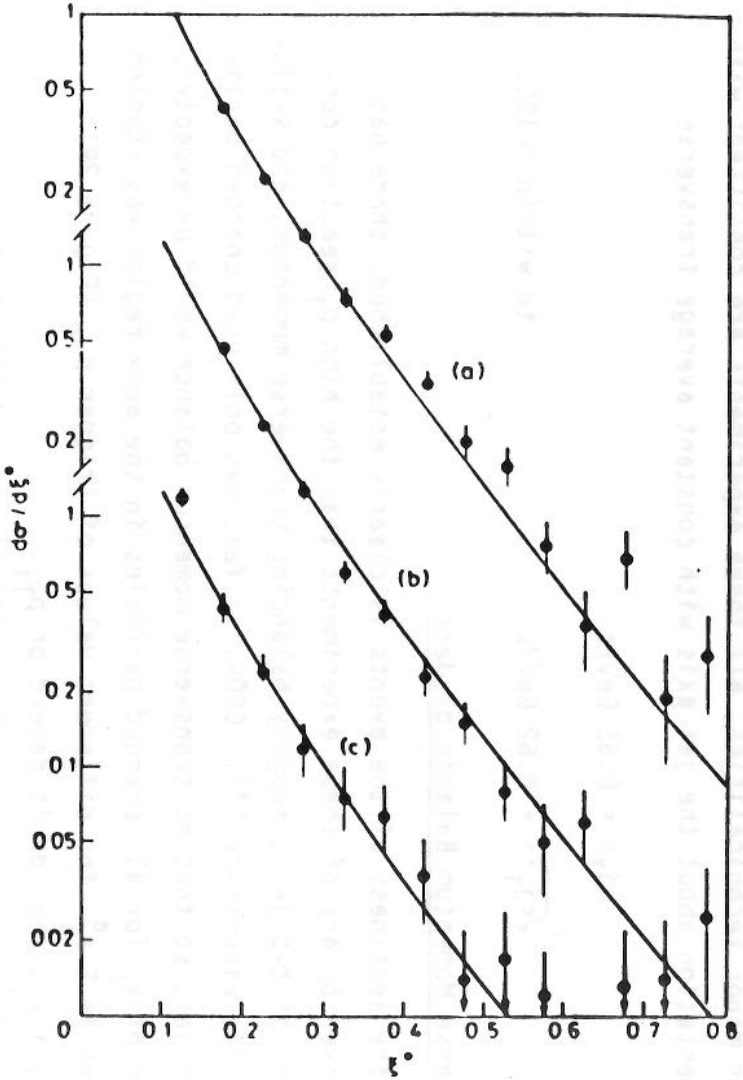

FIG. 31

the experiments have been in reasonable agreement. However, this does not seem to be the case with data on the fragmentation of trigger side jets. The data are contradictory among the various experiments, and also seemingly at variance with the concept of scaling in jet fragmentation [44].

The CERN-Saclay Group [45] define the same side jet as the vector sum of all neutrals with $p_T > 0.8$ GeV/c detected in their lead glass (Figure 1). They define the fragmentation variable ξ as the x_E of charged fragments referred to the neutral jet axis. The same side fragmentation distribution in the variable ξ is shown in Figure 31, corrected for the detector acceptance, for three intervals of p_{Tt} of the neutral jet: a) $5.0 \leq p_{Tt} \leq 6.0$ GeV/c, b) $6 \leq p_{Tt} \leq 8$ GeV/c, c) $p_{Tt} > 8$ GeV/c. The curves are a fit to a scaling form for the fragmentation function

$$\frac{d\sigma}{d\xi} = \frac{A}{\xi} \exp(-\xi/0.13) \quad ,$$

which agrees with the data for all three p_{Tt} intervals.

CCOR [24] look at the same question in a different way. They plot the distribution in transverse momentum p_T of all associated charged particles in the same side region [46], for three values of π^0 p_{Tt} (Figure 32). It appears from these data that the unscaled associated charged particle p_T distributions do not change as a function of trigger p_{Tt} in the range $2.5 \leq p_{Tt} \leq 8.0$ GeV/c. However, there is a big change relative to the zero threshold (minimum bias) trigger.

This effect can be seen in another way by plotting the average value of the sum of x_E for all charged particles in the same side region, $\langle \Sigma\, x_E^S \rangle$, as a function of p_{Tt} of the triggering π^0 (Figure 33). $\langle \Sigma\, x_E^S \rangle$ does not remain constant, as would be expected with a scaling fragmentation function, but instead decreases dramatically with increasing p_{Tt}. Note that the small values observed for the associated momentum fraction are as expected, since the π^0 trigger is biased in favor of jets in which a π^0 fragment has taken most of the momentum [44].

The data of the British-French-Scandinavian Group [32] seem to support CCOR rather than CERN-Saclay. For the same side charged particles associated with an identified charged particle trigger, BFS plot $\langle |\Sigma\, p_x^S| \rangle = \langle \Sigma\, x_E^S \rangle \times p_{Tt}$, as a function of trigger p_{Tt} (Figure 34). Although there is a component of $\langle |\Sigma\, p_x| \rangle$ that rises with p_{Tt}, the intercept is not zero at $p_{Tt} = 0$. Thus, we find

$$\langle \Sigma\, x_E^S \rangle = 0.03 + \frac{0.11}{p_{Tt}} \quad ,$$

which clearly exhibits non-scaling [47].

g) Contributions of Resonances to Trigger Side Jets

The resonance contribution to single particle inclusive triggers is expected to be suppressed by the parent-daughter factor [44,48]. For a given trigger

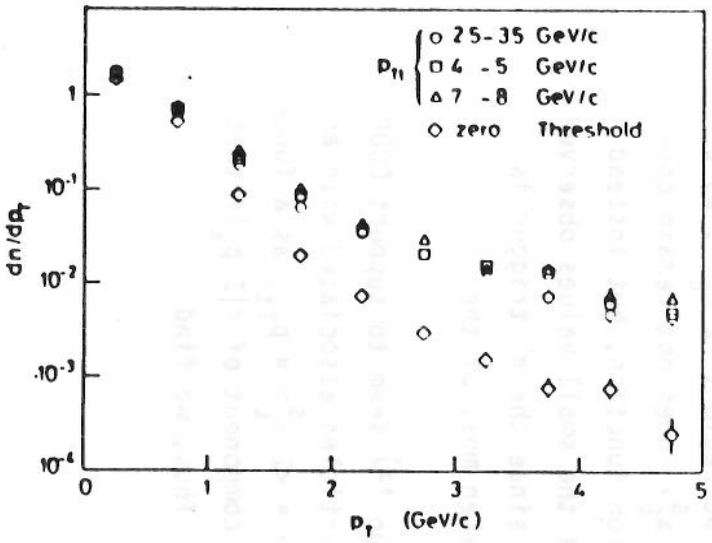

FIG. 32

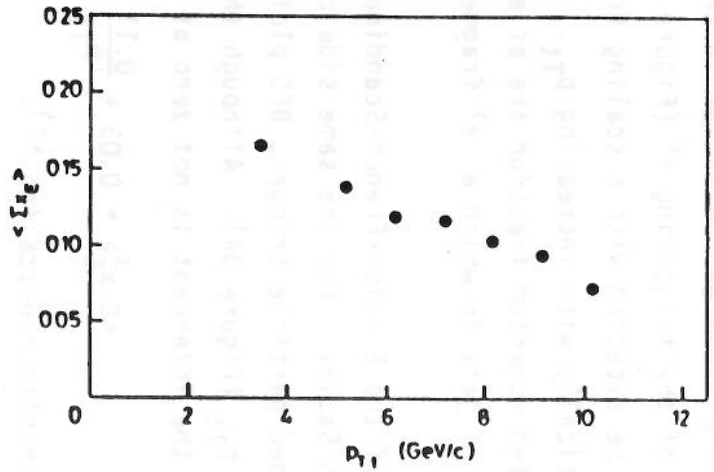

FIG. 33

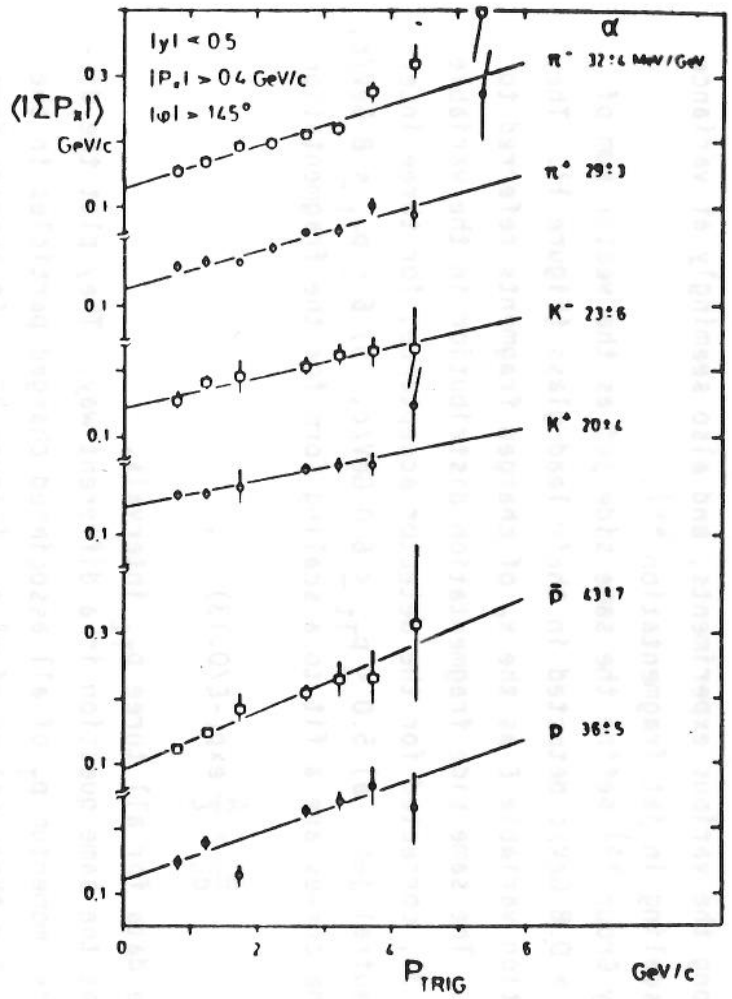

FIG. 34

transverse momentum p_{Tt}, a direct single particle is favored over the decay product of a higher transverse momentum resonance. This is nicely illustrated by an attempt of BFS [52] to understand what fraction of the trigger-side correlation effects (Figure 34) could be explained by the presence of resonances. The resonances are searched for by combining the trigger particle with other particles in the event. The results are shown in Figure 35, which appears at first sight to indicate lots of resonance production. However, the combinatorial background is suppressed in the figure. The resonances observed correspond to only $\sim 5\%$ of the triggers.

A similar effect is observed by CERN-Saclay [45] in a distribution of the momentum component of associated same side charged particles transverse to the axis of the neutral jet (Figure 36). This distribution disagrees slightly with their jet Monte Carlo calculation (solid line), especially at low values of transverse momentum, $j_{T\theta}$. However, this is no cause for alarm since the small effect can originate from a $\rho^{\pm}$ contribution to the sample. In Figure 37, the invariant mass distribution of charged hadron-neutral cluster pairs is shown for jets containing a single neutral cluster, under the assumption that both particles are pions. A clear, but small, bump at the ρ mass is visible in the data, which corresponds to only a very small fraction of the observed same side events. However, the inclusive ρ cross section required to produce this small effect is $(\rho^{+} + \rho^{-})/\pi^{0} = 1.0 \pm 0.5$ for $6 \leq p_T \leq 10$ GeV/c. This again illustrates the suppression of multi-body resonances in an inclusive single particle trigger.

IV - THE SEARCH FOR DIRECT SINGLE PHOTON PRODUCTION

Direct photon production at high p_T has recently become a "hot" topic because of the prediction [49] of "the inverse QCD Compton effect", i.e., the constituent reaction quark + gluon → quark + γ. The beauty of this reaction as a hadronic probe is that γ-rays are allowed to emerge freely from inside a hadron. Thus, no song-and-dance about jets and fragmentation is required. The high p_T QCD γ-rays from hadron collisions will emerge cleanly, unaccompanied by any other same-side particles. In fact, in the context of the QCD jet model, the observed ratio of, e.g., γ/π^{0} will be enhanced relative to the ratios of the constituent processes [49], since the π^{0}, as a fragment of a jet, will suffer a parent-daughter suppression [44] while the γ-ray will not.

Originally, direct photon production was proposed [50] as a mechanism to explain the copious yield of prompt leptons observed in hadron collisions [51]. Internal (Dalitz) conversion of the direct photons would produce the prompt leptons. A γ/π^{0} ratio of $\sim 10\%$ would be sufficient to explain the lepton/pion ratio of $\sim 10^{-4}$ observed for $p_T > 1.0$ GeV/c.

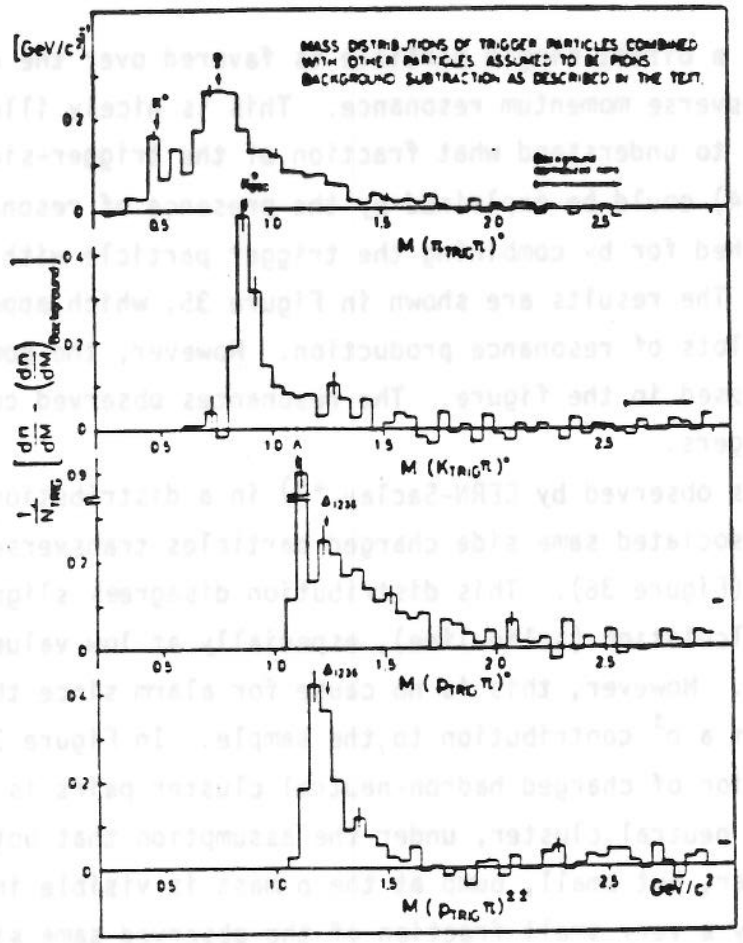

FIG. 35

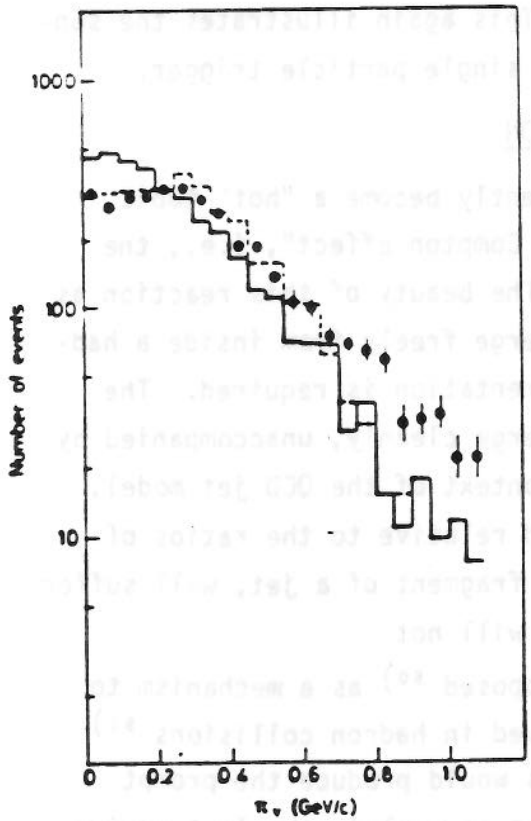

FIG. 36

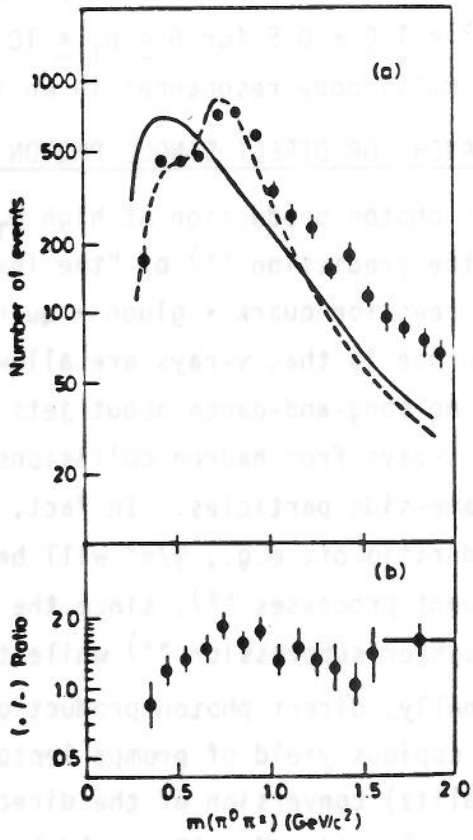

FIG. 37

Two early experiments at the ISR looked for direct photons. CCRS [52], as part of their direct electron measurements, searched for low mass e^+e^- pairs. An upper limit for e^+e^- pairs with mass $0.35 \leq m_{e^+e^-} \leq 0.45$ GeV/c^2, and $p_T > 1.3$ GeV/c was given, which can be converted to a 95% c.l. upper limit for real photons

$$\gamma/\pi^0 < 5\% \text{ for } p_T > 1.3 \text{ GeV/c} \quad .$$

A direct search for real photons by a CERN group produced the result [53]

$$\gamma/\pi^0 = 0.20 \pm 0.07 \pm 0.06 \text{ for } 2.8 \leq p_T \leq 3.8 \text{ GeV/c} \quad .$$

The 0.07 error comes from the uncertainty of the energy response curve of the lead glass detector, and the 0.06 from all the other sources of error. Note that the raw γ/π^0 signal observed was 0.46, which must then be corrected for single photon background from $\pi^0 \to \gamma\gamma$, $\eta^0 \to \gamma\gamma$ and other similar decays.

This year, significantly improved results have been obtained on the production of both real photons and low mass virtual photons in p-p collisions at the ISR. The CERN-Saclay-Zurich Group [54], in the same spectrometer used for π^0 production (Figure 1), have measured same side low mass e^+e^- pairs for $p_T > 1.6$ GeV/c. The invariant mass spectrum is shown in Figure 38. The background from various Dalitz decays, $\pi^0 \to \gamma e^+e^-$, $\eta^0 \to \gamma e^+e^-$, etc., is shown and is negligible for $m_{e^+e^-} > 0.500$ GeV/c^2. In addition to the peaks corresponding to $\rho^0 + \omega^0 \to e^+e^-$ and $\phi^0 \to e^+e^-$, a significant e^+e^- continuum, not due to known Dalitz decays, is observed in the mass range $0.400 \leq m_{e^+e^-} \leq 0.600$ GeV/c^2. The authors interpret this excess as being due to charmed particle production [55]; however, they also quote the upper limit of

$$\gamma/\pi^0 < 1.9\% \text{ at } p_T = 1.9 \text{ GeV/c} \quad ,$$

in case the effect were due to direct γ production. The vector meson production observed corresponds to cross sections

$$\frac{\rho^0 + \omega^0}{2\pi^0} = 0.59 \pm 0.20 \quad \text{for} \quad p_T > 2.0 \text{ GeV/c}$$

and

$$\frac{\phi^0}{\pi^0} = 0.12 \pm 0.05 \quad \text{for} \quad p_T > 2.1 \text{ GeV/c} \quad .$$

Measurements on low mass e^+e^- pairs were also reported by the BCSAY collaboration [56]. The apparatus, which contained lithium/xenon transition radiation detectors and liquid argon calorimeters, has already been discussed (Figure 10). The invariant mass distribution of the observed electron pairs is shown in

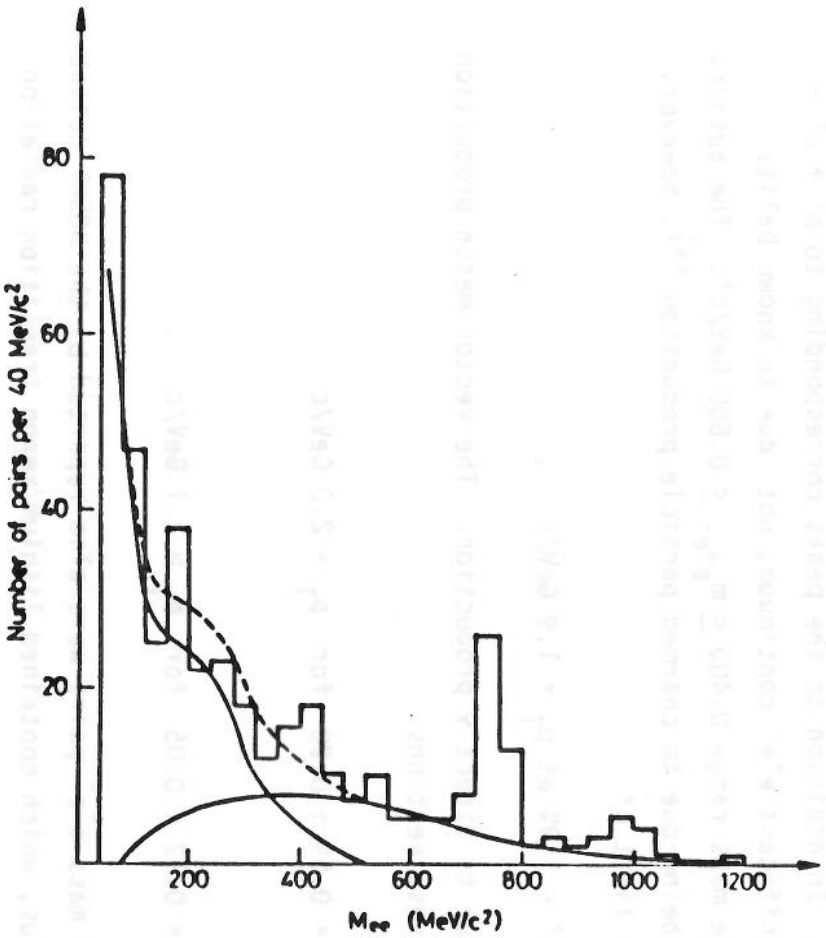
Number of pairs per 40 MeV/c²
80
60
40
20
200
400
600
800
1000
1200
Mee (MeV/c²)

FIG. 38

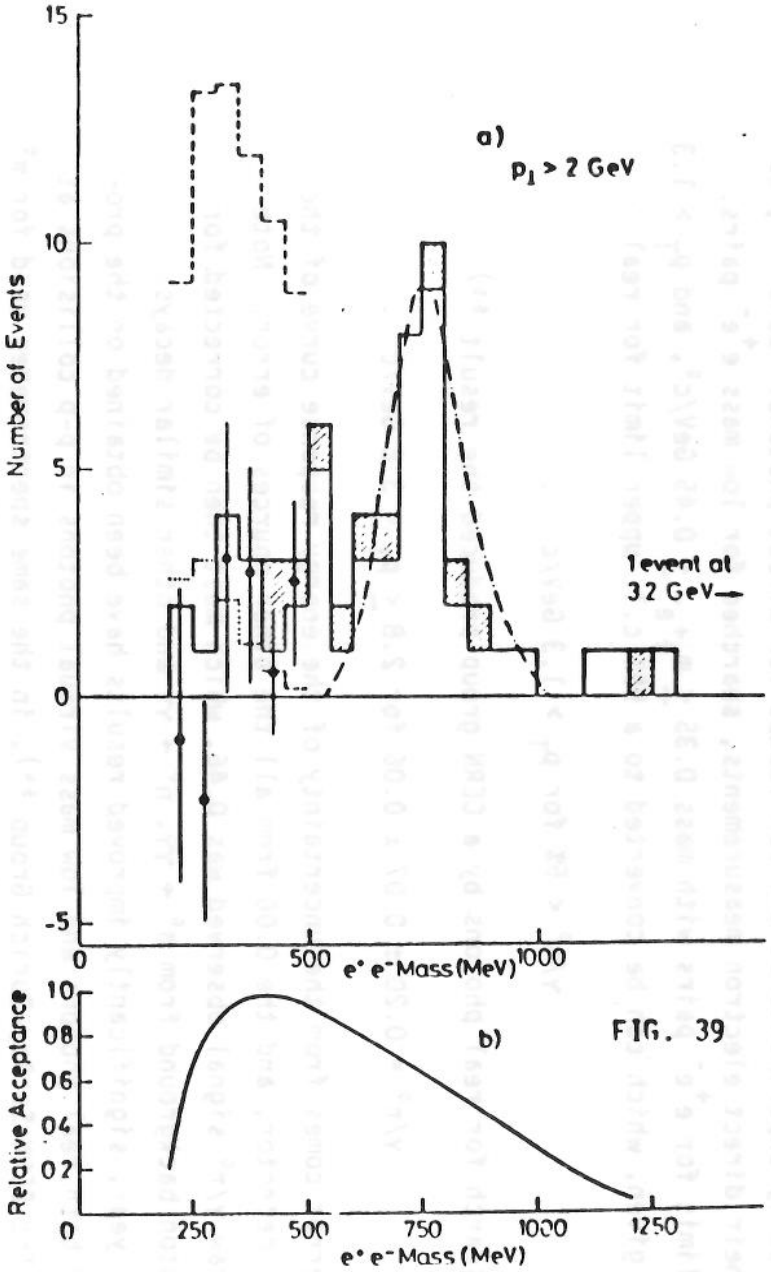
a)
p⊥ > 2 GeV
Number of Events
15
10
5
0
-5
1 event at
32 GeV
500
e⁺e⁻ Mass (MeV)
1000
b)
Relative Acceptance
10
08
06
04
02
0
250
500
750
1000
1250
e⁺e⁻ Mass (MeV)

FIG. 39

Figure 39a for pairs with $2.0 < p_T < 3.0$ GeV/c. The spectrum has not been acceptance corrected, but the acceptance is shown in Figure 39b. A clear peak from the ρ^0 and $\omega^0 \rightarrow e^+e^-$ is observed as well as a continuum for masses $0.25 \leq m_{ee} \leq 0.50$ GeV/c^2. The dotted line shows the prediction for all known Dalitz decays, and the dot-dash line the expected shape from the tails of the ρ^0 and ω^0. The data points represent the difference between the measured continuum and the Dalitz and ρ^0, ω^0 contributions. The dashed line at the top left side shows the prediction for low mass pairs corresponding to $\gamma/\pi^0 = 10\%$. The conclusion is that

$$\gamma/\pi^0 \leq (0.55 \pm 0.92)\% \quad \text{for} \quad 2.0 \leq p_T \leq 3.0 \text{ GeV/c} \quad .$$

Thus, all the low mass virtual photon experiments are in agreement.

Results from an exceedingly difficult real photon search at $\sqrt{s} = 53.2$ GeV were published this year by the Rome-Brookhaven-CERN-Adelphi Group [57]. The detector consisted of a matrix of 9 by 15 lead glass blocks, 10×10 cm^2 in area and 35 cm long, placed behind two matrices of scintillation counters which allowed the rejection of charged particles. The whole detector was remotely moveable between $\sim$1.5 and 4.5 meters from the interaction point so that systematic effects due to the geometry could be studied. As the authors most eloquently explain, "The most delicate points in the search for single gamma ray direct emission are of two different types. The first is the danger of interpreting a gamma produced in the decay of a π^0 or η^0 as a single gamma ray either because its companion is not observed in the solid angle of the apparatus above the energy threshold of the counters or because the two gamma rays are not geometrically resolved. The second delicate problem is the background due to anti-neutrons annihilating in the lead glass with a large fraction of the energy emitted as π^0's."

The results of the direct γ measurement are shown in Figure 40 as a function of p_T. It should be noted that the direct γ signal extracted after background corrections corresponds to only $\sim$10% of the observed single photon signal. The black line shown is a QCD prediction [38]. It is not clear whether the data support the QCD prediction or are consistent with a zero value for γ/π^0. However, one definite conclusion from the data is that to 95% confidence

$$\gamma/\pi^0 < 5\% \quad \text{for} \quad 2.3 \leq p_T \leq 3.4 \text{ GeV/c} \quad ,$$

which is in substantial disagreement with the previous real photon result [53].

Another point worthy of note is that the QCD predictions are ambiguous. For instance, Contogouris, et al [58], agree with Field's calculation [38] (Figure 40) if they use scale invariant distributions for the quarks and gluons.

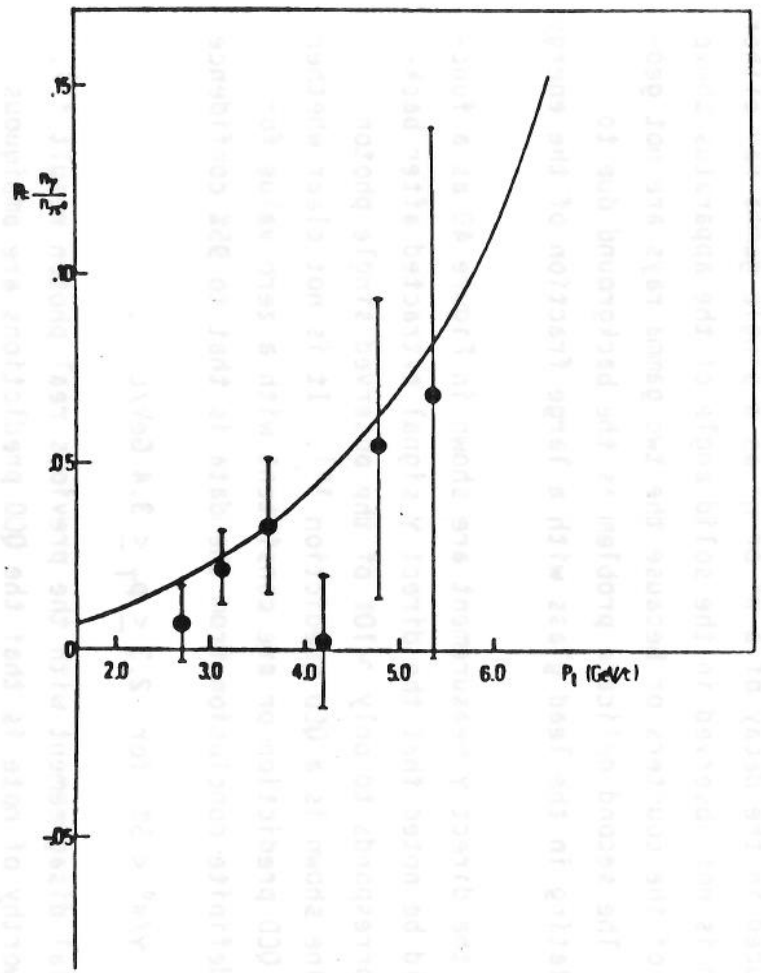
.15
.10
.05
0
-.05
2.0
3.0
4.0
5.0
6.0
P_t (GeV/c)

FIG. 40

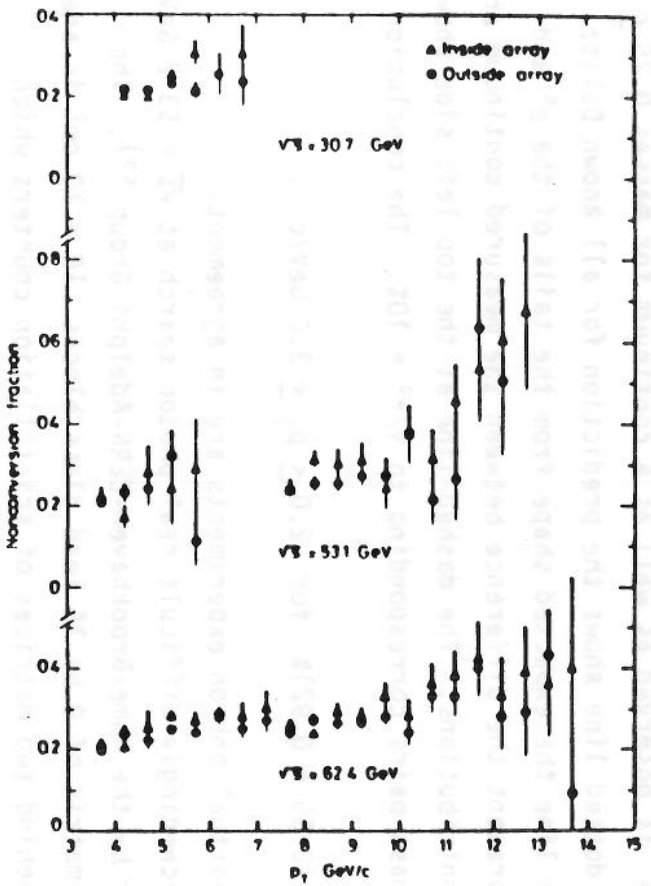
Inside array
Outside array
√s = 30.7 GeV
√s = 53.1 GeV
√s = 62.4 GeV
Nonconversion fraction
p_T GeV/c

FIG. 41

However, if they include QCD scale violating effects in these distributions, the predicted γ yield drops by an order of magnitude at high p_T to a value of γ/π^0 which never exceeds 5% for $2.0 \leq p_T \leq 16.0$ GeV/c! Obviously, this is a difficult challenge for experimenters.

As a parting remark, I shall take note of a crude attempt by CCOR [18] to overcome the problem of not being able to geometrically resolve the two γ-rays from a π^0. It was noted previously [20] that the π^0 data of Figure 4 were consistent with all being due to two γ-rays. This was determined by measuring the fraction of events for which no γ-ray conversion in the coil was indicated. The non-conversion fraction is plotted in Figure 41 as a function of p_T. For pure two γ-ray events, a value of 25% is expected, for pure single γ, 50%, and, e.g., for 1/3 single γ and 2/3 two γ, 33%. The conclusion from Figure 41 is that for $4.0 \leq p_T \leq 10.5$ GeV/c and $\sqrt{s}$=62.4 GeV, $\gamma/\pi^0 < 50\%$. Above 10.5 GeV/c, the data are inconclusive. It is hoped to improve significantly on this attempt in the near future.

V - CONCLUSION

Many beautiful results on high p_T physics have been obtained this past year. A new regime of physics seems to be indicated for $p_T > 7.5$ GeV/c. Clear indications of jet structure abound. QCD, coupled with the quark-parton model, provides a reasonable framework for interpreting the data. However, many questions remain unanswered. For example:

(i) Is the p_T^{-8} behavior at "intermediate" p_T due to quark transverse momentum [12], quark-meson scattering [7], both, or neither? What will happen at even higher p_T and $\sqrt{s}$?

(ii) Why does the "effective" quark transverse momentum $\langle k_T \rangle$ seem to increase with p_T, while the mean width of the jet fragmentation $\langle j_T \rangle$ appears to remain constant?

(iii) Why do hadronic induced jets appear to have larger mean fragmentation transverse momentum $\langle j_T \rangle$ than jets from e^+e^- annhilation [41]?

(iv) At high p_T, is there really a two-jet system that satisfies the quasi-elastic kinematics of constituent scattering?

(v) Is there evidence for two species of jets: quark and gluon?

(vi) Are constituent distributions and fragmentation functions in purely hadronic collisions really related to those determined in electromagnetic and weak interactions? What are their scaling properties?

(vii) Can direct photon production via the inverse QCD compton effect [49] be reliably calculated or measured?

(viii) Will QCD ever be able to calculate the bound-state quark wave functions inside hadrons so that the quark-parton model, effective $\langle k_T \rangle$, and other phenomenology can be eliminated?

(ix) If high p_T particle production is really the result of a quark being struck with momentum transfers in excess of $q^2 = 400\ GeV^2/c^2$, how hard must a quark be hit before it is able to escape from its hadronic confines and emerge intact into the real world?

Furthermore, there are many other issues and beautiful data in high p_T physics that I haven't been able to mention for want of time and space.

NOTES and REFERENCES

1. M.J. Tannenbaum, "High p_T Processes - Experimental Aspects", in Proceedings of the Meeting in Marseilles on Hadron Physics at High Energies, June 1978, edited by C. Bourrely, J.W. Dash and J. Soffer (Centre de Physique Theorique C.N.R.S. - F-13288, Marseille, France).
2. F.W. Büsser et al., Phys. Lett. 46B, 471 (1973).
3. F.W. Büsser et al., Nucl. Phys. B106, 1 (1976).
4. K. Eggert et al., Nucl. Phys. B98, 49 (1975).
5. D. Antreasyan et al., Phys. Rev. Lett. 38, 112 (1977).
6. S.M. Berman, J.D. Bjorken, J. Kogut, Phys. Rev. D4, 3388 (1971); S.M. Berman and M. Jacob, Phys. Rev. Lett. 25, 1683 (1970); J.D. Bjorken, Phys. Rev. D8, 4098 (1973).
7. R. Blankenbecler, S.J. Brodsky and J.F. Gunion, Phys. Rev. D6, 2652 (1972); Phys. Lett. 42B, 461 (1972); Phys. Rev. D12, 3469 (1975); ibid. D18, 900 (1978). See also, S.J. Brodsky and G.R. Farrar, Phys. Rev. Lett. 31, 1153 (1973); Phys. Rev. D11, 1309 (1975).
8. J. Kogut, D.K. Sinclair and L. Susskind, Phys. Rev. D7, 3637 (1973); J. Kogut, G. Frye and L. Susskind, Phys. Lett. 40B, 469 (1972).
9. S.D. Ellis and M.B. Kislinger, Phys. Rev. D9, 2027 (1974).

10. R.D. Field and R.P. Feynman, Phys. Rev. D15, 2590 (1976); R.P. Feynman, *Photon-Hadron Interactions*. (Benjamin, Reading, Mass. 1972); R.P. Feynman, R.D. Field and G.C. Fox, Nucl. Phys. B128, 1 (1977); Phys. Rev. D18, 3320 (1978).
11. R.F. Cahalan, K.A. Geer, J. Kogut and L. Susskind, Phys. Rev. D11, 1199 (1975).
12. R.D. Field, Phys. Rev. Lett. 40, 997 (1978).
13. R. Cutler and D. Sivers, Phys. Rev. D16, 679 (1977); ibid. D17, 196 (1978).
14. B.L. Combridge, J. Kripfganz and J. Ranft, Phys. Lett. 70B, 234 (1977).
15. A.P. Contogouris, R. Gaskell and S. Papadopoulos, Phys. Rev. D17, 2314 (1978).
16. J.F. Owens, E. Reya and M. Gluck, Phys. Rev. D18, 1501 (1978); J.F. Owens and J.D. Kimel, ibid. 3313 (1978).
17. A.G. Clark et al., Phys. Lett. 74B, 267 (1978).
18. A.L.S. Angelis et al., Phys. Lett. 79B, 505 (1978).
19. Although evident from the figure, this was first pointed out to me by Mel Shochet via Bernard Pope, and confirmed by Pierre Darriulat.
20. By observing the fraction of events in which a γ-ray conversion in the 1 X_0 thick coil is detected in the hodoscope of scintillation counters (B) located just outside the solenoid, it is concluded that the results of Figure 4 are consistent with all being due to two photons. These could be from η^0 mesons as well as π^0 mesons. However, no correction was applied to the data since the η^0 cross section is unknown in this p_T range. In any case, the correction is probably small and independent of p_T and $\sqrt{s}$. For instance, if η^0/π^0 were 0.55, as measured at lower values of p_T [2], the cross sections would have to be corrected by -17%.
21. The sharp eyed observer will note that in Figure 6 a value of n is given at x_T=0.25, where there are no data at $\sqrt{s}$=53.1 GeV. Since good data exist on both sides of this gap, it is quite easy to make a decent interpolation using only a ruler. Alternatively, at each value of $\sqrt{s}$, the cross sections deviate only slightly from a power law so that it is very easy to make a separate fit to the data for each value of $\sqrt{s}$. For instance, a fit of the form

$$E\frac{d^3\sigma}{dp^3} = \frac{A}{p_T^{\alpha}(1+x_T)^{\beta}}$$

gives results:

$\sqrt{s}$ (GeV)	x_T Range	A cm^2/GeV^2	α	β	χ^2/d.o.f.
62.4	0.12 to 0.45	1.86 E-27	7.02	14.53	30/18
53.1	0.13 to 0.49	9.01 E-27	8.57	9.32	14/13
30.6	0.26 to 0.46	4.3 E-27	7.1	18.3	6/3

These fits by themselves don't tell you any physics. However, they can be used with Equation (4) to give $n(x_T)$ for any value of x_T within the range of the fit.

22. Fits to the entire p_T range of the 53.1 and 62.4 GeV data using a sum of two terms of the form of Equation (6) with six independent parameters give χ^2 of over 61 for 31 d.o.f., compared with a total χ^2 of 28 for 31 d.o.f. for the independent fits above and below p_T=7.5 GeV/c. In order to definitively answer the question of whether the sum of two scaling terms is excluded by the data, it would be nice to fill the gap in the 53.1 GeV data (Figure 5) which occurs right in the transition region.
23. e.g., see the discussion by J. Bjorken et al., in Proceedings of the 1971 International Symposium on Electron and Photon Interactions at High Energies, edited by N.B. Mistry, (Laboratory of Nuclear Studies, Cornell University, Ithaca, N.Y., 1972), pp. 296-297.
24. A.L.S. Angelis et al., "Results on Correlations and Jets in High Transverse Momentum p-p Collisions at the CERN ISR," CERN preprint submitted to the XIX International Conference on High Energy Physics, Tokyo (1978).
25. e.g., compare to Pisa-Stony Brook results at lower p_{Tt}, G. Finocchiaro et al., Phys. Lett. 50B, 396 (1974).
26. e.g., see L. Di Lella, "Correlations in High p_T Final States," in Proceedings of the XVII International Conference on High Energy Physics, edited by J.R. Smith, (S.R.C., Rutherford Laboratory, Chilton, Didcot, UK, 1974), pp. v-17 to v-19.
27. J.H. Cobb et al., Phys. Rev. Lett. 40, 1420 (1978); M. Goldberg et al., "Correlations of High Transverse Momentum π^0 Pairs Produced at the CERN ISR." (to be submitted to Nucl. Phys. B.)
28. G. Sterman and S. Weinberg, Phys. Rev. Lett. 39, 1436 (1977).
29. P. Darriulat et al., Nucl. Phys. B107, 429 (1976).
30. M. Della Negra et al., Nucl. Phys. B127, 1 (1977).
31. M. Jacob and P.V. Landshoff, Nucl. Phys. B113, 395 (1976).
32. M.G. Albrow et al., Nucl. Phys. B145, 305 (1978).
33. see FFF, Reference 10.
34. see also, E.M. Levin and M.G. Ryskin, Leningrad Preprints, 1975 and 1976, as quoted by P. Darriulat, Rapporteur's talk, in Proceedings of the XVIII International Conference on High Energy Physics, Tbilissi, 1976, edited by N.N. Bogolubov et al., (JINR, Dubna, U.S.S.R., 1976).

35. Note that for distributions that give Gaussian projections on two orthogonal axes x and y with $\langle x^2\rangle=\langle y^2\rangle\equiv\sigma^2$, then $\langle|x|\rangle=\langle|y|\rangle = \sigma\sqrt{2/\pi}$. The distribution in the radial coordinate $r=\sqrt{x^2+y^2}$ is not Gaussian but is exponential in r^2 [$dp=e^{-r^2/2\sigma^2}\, dr^2/2\sigma^2$] so that

$$\langle r^2\rangle = \langle x^2\rangle + \langle y^2\rangle = 2\sigma^2$$
$$\langle r\rangle = \sigma\sqrt{\pi/2}$$
$$\langle|x|\rangle^2 + \langle|y|\rangle^2 = 8\langle r\rangle^2/\pi^2 = 2\langle r^2\rangle/\pi$$

36. The same relation with all quantities rms is also valid.
37. Note that I did not take the CCOR Tokyo data from Figure 20, but used a later version which has ∿10% to 20% lower values of $\langle|p_{out}|\rangle$.
38. R.D. Field, Report CALT-68-688, invited talk presented at the Symposium on Jets in High Energy Collisions, Niels Bohr Institute - Nordita, Copenhagen, July 1978 (to be published in Physica Scripta).
39. CERN/ISRC/77-24, "Status Report on Experiment R-108," ISRC Committee Document (private communication not for distribution or publication).
40. n.b. This is just another way of saying that $\langle|k_T|\rangle \gg \langle|j_{T\phi}|\rangle$, so that the width of the away azimuthal distribution is dominated by k_T for large values of associated particle transverse momentum.
41. Note that $\langle j_T\rangle$ values quoted for hadron collisions are observed for jet fragments with $p_T > 2.0$ GeV/c (CCOR, Figure 26), $p_T > 0.8$ GeV/c (CERN-Saclay, Figure 27), and $p_T > 1.0$ GeV/c (BFS, Figure 28). In all three cases, the jets have $|\Sigma\, \vec{p}_T| > 3$ GeV/c. For the jets in e^+e^- collisions, G. Zech, in these proceedings, quotes $\langle j_T\rangle \approx 0.35$ GeV/c integrated over all charged particle momenta. However, for a fixed e^+e^- CM energy, the $\langle j_T\rangle$ is observed to increase with increasing momentum of the jet fragments.
42. A.G. Clark et al., "Large Transverse Momentum Jets in High Energy p-p Collisions," CERN preprint submitted to the XIX International Conference on High Energy Physics, Tokyo (1978).
43. See, however, FERMILAB-Lehigh-Pennsylvania-Wisconsin Group: W. Selove, these proceedings; A.R. Erwin, Report COO-088-36, 1978, presented at the Vanderbilt Conference on New Results in High Energy Physics.
44. e.g., see a nice treatment in M. Jacob and P.V. Landshoff, "Large Transverse Momentum and Jet Studies." (to be published in Physics Reports).
45. A.G. Clark et al., "Experimental Study of the Fragmentation of Large Transverse Momentum Jets in High Energy p-p Collisions," CERN preprint submitted to the XIX International Conference on High Energy Physics, Tokyo (1978).

46. This is not strictly true; charged tracks in a 7° half angle cone around the triggering π^0 are excluded. CERN-Saclay [45] have investigated the effect on their data of excluding charged tracks within a 3° cone about the trigger and have found no effect.

47. Note that the values of $\langle \Sigma x_E \rangle$ deduced from Figure 34 are only about half those reported by CCOR (Figure 33). This is not unreasonable since the BFS same side solid angle is $|y| < 0.5$, $\Delta\phi = \pm 35°$, which is less than half that of CCOR. Also, CCOR cut on associated transverse momentum $p_T > 0.30$ GeV/c while for Figure 34, BFS require $|p_x| > 0.40$ GeV/c (see Figure 14).

48. Note that this factor can sometimes work the other way as in the decay of a very heavy particle into two light particles; e.g., see the discussion of the effect of $\psi(3.1) \to e^+e^-$ on the inclusive single electron spectrum, in Reference 52.

49. H. Fritzsch and P. Minkowski, Phys. Lett. 69B, 316 (1977).

50. G.R. Farrar and S.C. Frautschi, Phys. Rev. Lett. 36, 1017 (1976); see also, C.O. Escobar, Nucl. Phys. B98, 174 (1975); and E.L. Feinberg, Nuovo Cimento 34A, 391 (1976).

51. G.B. Bondarenko et al., in Proceedings of the 16th International Conference on High-Energy Physics, Chicago-Batavia 1972, edited by J.D. Jackson and A. Roberts (National Accelerator Laboratory, Batavia, Ill., 1973), Vol. 2, p. 328; J.P. Boymond et al., Phys. Rev. Lett. 33, 112 (1974); J.A. Appel et al., ibid. 722 (1974); F.W. Büsser et al., Phys. Lett. 53B, 212 (1974).

52. F.W. Busser et al., Nucl. Phys. B113, 189 (1976).

53. P. Darriulat et al., Nucl. Phys. B110, 365 (1976).

54. A. Chilingarov et al., "Production of High p_T Low Mass e^+e^- Pairs in High Energy p-p Collisions," CERN Preprint submitted to the XIX International Conference on High Energy Physics, Tokyo (1978).

55. T. Modis, these proceedings.

56. J.H. Cobb et al., Phys. Lett. 78B, 519 (1978).

57. E. Amaldi et al., Phys. Lett. 77B, 240 (1978); and I.N.F.N.-Rome Preprint n.113 (submitted to Nucl. Phys. B).

58. A.P. Contogouris, S. Papadopoulos and M. Hongoh, "Scale Violation Effects in Large p_T Direct Photon Production," McGill University Preprint (to appear in Phys. Rev. D, 1 May 1979).